Title
Control of transverse wakefields via phase-matched laser modes in parabolic plasma channels

Journal
Physics of Plasmas, 26(1)

ISSN
1070-664X

Authors
Djordjević, BZ
Benedetti, C
Schroeder, CB
et al.

Publication Date
2019

DOI
10.1063/1.5064740

Peer reviewed

This manuscript was accepted by Phys. Plasmas. Click here to see the version of record.

Control of transverse wakefields via phase-matched laser modes in parabolic plasma channels

B.Z. Djordjević,[1,2] C. Benedetti,[2] C.B. Schroeder,[2] E. Esarey,[2] and W.P. Leemans[1,2]
[1)] *Department of Physics, University of California, Berkeley, CA, 94720, USA*
[2)] *BELLA Center, Lawrence Berkeley National Laboratory, Berkeley, CA, 94720, USA*

The use of higher-order modes is proposed to control the transverse wakefield structure generated by a laser pulse propagating through a plasma channel. This can be done in the quasilinear regime in both the Laguerre-Gaussian and Hermite-Gaussian bases for appropriate laser-plasma parameters, independently of the longitudinal field. Control of the wake can be achieved by using modes of different mode numbers but with matched phase velocities to generate tunable, matched laser propagation. The wake can be tuned by modifying the initial phase and amplitude of each mode. In addition, it is shown that two different higher order modes can propagate at the same group velocity by appropriately tuning the frequencies. Geometric and frequency tuning of the laser driver allows for greater control of the transverse phase-space of the accelerated electron bunch.

I. INTRODUCTION

Experimental advances in the development of laser-plasma accelerators (LPAs) over the past two decades have verified theoretical predictions and promise new technological applications.[1,2] Of primary interest is the use of LPAs for a future collider design.[3,4] Likewise, there is great interest in using the technology for compact and brilliant X-ray light sources in the relatively near future.[5] Currently, LPA technology has been able to achieve accelerating gradients in excess of 100 GV/m and electron bunches with an energy of several GeV over centimeter-length scales.[6] Development of the field has been primarily enabled and driven by rapidly advancing laser technology.

Ultra-short, femtosecond scale pulses used in LPA experiments are often assumed to have a Gaussian transverse profile. In reality this is seldom the case and higher-order mode content is often present, which complicates laser pulse evolution in a plasma and can lead to reduced energy gains and potential bunch loss.[6,7] However, higher-order laser modes can be intentionally utilized and have been proposed in several advanced concepts, such as plasma undulators,[8–10] higher harmonic generation,[11] ring-shaped electron bunches,[12,13] and independent control of the focusing fields.[14] Ref. 14 explored the use of two modes to modify the transverse electric fields of the wake. In this paper we extend that concept by considering the fact that higher-order modes can be matched with respect to both their phase and group velocities by choosing the appropriate geometric mode indices as well as propagating modes of different laser frequencies. This velocity matching avoids slippage and mode beating, which can otherwise limit the laser-plasma interaction length.

In this paper we propose the utilization of higher-order Laguerre-Gaussian and Hermite-Gaussian modes to control the wake properties in an LPA. In most cases the presence of higher-order modes will lead to mode beating and thereby is detrimental to the purpose of guiding and accelerating a trailing bunch.[14] However, as described in this work, it is possible to select which modes are present in such a way that there will be no beating. Given the dispersion relation, one can select geometric mode numbers such that different modes have the same group and phase velocities, resulting in a superposition of those modes without beating. In this paper we consider the application of this idea to guiding elliptical bunches and verify its properties in the quasi-linear limit with particle tracking to model the bunch. Another issue we address is the fact that modes of different, non-complementary mode number propagate at different group velocities. This can be addressed by considering modes of different frequencies and is considered in the case where it is desired to reduce the electric field gradient near the axis.

In an LPA, a short and intense ($I > 10^{18}$ W/cm^2) laser pulse propagates through a plasma and generates a plasma wave.[2] If the length of the pulse, L, is approximately that of the plasma wavelength, $\lambda_p = 2\pi/k_p = 2\pi c/\omega_p$, where k_p is the plasma wavenumber, c is the speed of light, $\omega_p^2 = 4\pi n_0 e^2/m_e$ is the plasma frequency, n_0 is the on-axis plasma density, and e and m_e are the electron charge and mass, then a plasma wave will be resonantly excited by the ponderomotive force of the laser, $F \sim \nabla a^2$, where $a = eA/(m_e c^2)$ is the normalized amplitude and A is the vector potential of the laser field. The electric field of this wake, in the quasilinear regime $a \lesssim 1$, is proportional to the gradient of the intensity, $\vec{E} \sim \nabla a^2$, and this field is used to focus and accelerate an electron bunch. In a vacuum, the laser pulse will diffract on length scales on the order of the Rayleigh range, $Z_R = \pi r_0^2/\lambda$, where r_0 is the characteristic spot size of the laser, (i.e., where $I(r_0) = I_0/\mathrm{e}^2$), $\lambda = 2\pi/k \simeq 2\pi c/\omega$ is the laser wavelength, k is the laser wavenumber, and ω is the frequency of the laser. If r_0 is matched to the characteristic radius of curvature of the plasma channel then the pulse will be matched, meaning that it propagates with constant spot size r_0 and constant normalized amplitude a. The critical channel depth for matched guiding, assuming a parabolic plasma profile and low-power, low-intensity Gaussian laser, is given by $\Delta n_c = (\pi r_e r_0^2)^{-1}$,

where $r_e = e^2/m_e c^2$ is the classical electron radius.

The transverse dynamics of a bunch as it is accelerated can be described by the rms spot size equation, $d^2\sigma/dz^2 + k_\beta^2\sigma - \epsilon_n^2/(\gamma^2\sigma^3) = 0$, where σ is the rms spot size of the electron bunch, ϵ_n is the normalized emittance, $k_{\beta_x}^2 = k_p \lim_{x\to 0}[(E_x - B_y)/(\gamma E_0)]/x$ is the betatron wavenumber, $\gamma = 1/\sqrt{1 - v^2/c^2} = \sqrt{1 + p^2/(m_e c)^2}$ is the relativistic Lorentz factor, and $E_0 = m_e c\omega_p/e$ is the cold, nonrelativistic wave breaking field. Typically plasma-based accelerators have very strong focusing fields and these can lead to large betatron oscillations in the accelerated electron bunch.[15] Controlling the focusing forces is highly desirable. For electron acceleration, steep electric field gradients can lead to small bunch size and a dense bunch can lead to ion motion.[16,17] For positron acceleration the steep gradients yield dense bunches that blow-out the plasma electrons and expose the positron bunch to defocusing by the background ions.[13,18] An additional complication for LPAs is that there has not been an easy way to control the transverse emittances ϵ_x and ϵ_y independently. This will be important for future colliders since final focus emittance ratios as high as $\epsilon_x/\epsilon_y = 100$ are considered to mitigate beam-beam effects at the interaction point.[19] The use of higher-order modes in the laser driver provides a solution to these challenges.

This paper is organized as follows. In Sec. II we present the general solutions to the paraxial wave equation in Cartesian and cylindrical coordinates as well as the propagation of multiple, overlapping modes in a plasma channel, which typically results in mode beating. The dependence of the phase and group velocities on mode number and laser wavenumber is presented. In Sec. III we present our analysis regarding geometric tuning of the transverse wakefield. It is shown that for Hermite as well as for Laguerre-Gaussian modes, one can independently alter the transverse electric fields in the x and y directions without altering the longitudinal accelerating field. In Sec. IV we show that the frequencies of two different modes, whether of orthogonal polarization or temporal separation, can be chosen so that the modes propagate at the same group velocity. This model is then verified using particle tracking to show that a higher-order mode can be used to reduce the transverse electric field gradients and allow for the acceleration of wider bunches than possible for a Gaussian laser driver while keeping the bunch emittance constant. In Sec. V we present a summary of our analysis and describe potential future directions and experiments.

II. HIGHER-ORDER LASER MODE PROPAGATION IN A PLASMA CHANNEL

Laser pulse propagation through a plasma channel can be analyzed in the low-power and low-intensity limit $|a|^2 \ll 1$, assuming the paraxial approximation in the direction of propagation, $|k\partial_z a| \gg |\partial_z^2 a|$, by the paraxial wave equation:

$$\nabla_\perp^2 a + 2ik\partial_z a = k_p^2(n/n_0)a, \tag{1}$$

where we have the Laplacian $\nabla_\perp^2 = \partial_x^2 + \partial_y^2$ in Cartesian coordinates, $\nabla_\perp^2 = (1/r)\partial_r(r\partial_r) + (1/r^2)\partial_\theta^2$ in cylindrical coordinates, $r = \sqrt{x^2 + y^2}$, and $\theta = \arctan(y/x)$. The plasma density n is given by a parabolic channel with a radius of curvature (critical depth) matched to the initial laser spot size r_0:

$$n(r) = n_0\left(1 + \frac{4}{k_p^2}\frac{r^2}{r_0^4}\right). \tag{2}$$

In Eqs. (1) and (2) we are neglecting the effects of relativistic self-focusing and ponderomotive self-channeling. It is well known that when a low-power, low-intensity Gaussian pulse is injected into a matched parabolic channel that the spot size, r_s, and peak intensity a_0^2 will remain constant.[2] This can be extended to the quasilinear regime by considering the effects of relativistic self-focusing.[2] This matching criterion can also be extended to any individual higher-order Hermite or Laguerre-Gaussian mode including plasma wave guiding effects.[20]

A. Cartesian geometry

In the Cartesian coordinate system, the solution to the paraxial wave equation, Eq.(1), corresponding to matched laser propagation, is of the following form for arbitrary horizontal and vertical mode numbers m and n,

$$a_\perp(x,y,z) = \frac{a_{m,n}}{(m!n!2^{m+n})^{\frac{1}{2}}} H_m\left(\frac{\sqrt{2}x}{x_0}\right) H_n\left(\frac{\sqrt{2}y}{y_0}\right) \times e^{-\frac{(x^2+y^2)}{r_0^2}} e^{i(\varphi_{mn}+\varphi_0)}, \tag{3}$$

where $a_\perp$ is the perpendicular component of a, $a_{m,n}$ is the amplitude contribution of mode (m,n) to the radiation field, H_m is the Hermite polynomial of order m, $x_0 = y_0 = r_0$ are the spot sizes, the phase contribution from the dispersion relation is given by $\varphi_{mn} = (-1/2k)[k_p^2 + 4(m+n+1)/r_0^2]z$, and the initial phase is φ_0. From this we derive the phase velocity of the mode:[21]

$$\frac{v_{p,H}}{c} = 1 + \frac{1}{2k^2}\left[k_p^2 + \frac{4(m+n+1)}{r_0^2}\right]. \tag{4}$$

B. Cylindrical geometry

In the cylindrical coordinate system, the solution for the transverse field to Eq. (1) for matched propagation

This manuscript was accepted by Phys. Plasmas. Click here to see the version of record.

and arbitrary radial and azimuthal mode numbers μ and ν is given by

$$a_\perp(r,\theta,z) = a_{\mu\nu}\sqrt{\frac{2\mu!}{\pi(\mu+\nu)!}}\left(\frac{\sqrt{2}r}{r_0}\right)^\nu L_{\mu\nu}\left(\frac{2r^2}{r_0^2}\right) \times e^{-\frac{(x^2+y^2)}{r_0^2}} e^{i(\varphi_{\mu\nu}+\varphi_0+\nu\theta)}, \tag{5}$$

where $L_{\mu\nu}$ is the Laguerre polynomial of radial order μ and azimuthal order ν and θ is the azimuthal angle. The modal phase contribution is given by $\varphi_{\mu\nu} = (-1/2k)[k_p^2 + 4(2\mu+\nu+1)/r_0^2]z$ and the phase velocity is:

$$\frac{v_{p,L}}{c} = 1 + \frac{1}{2k^2}\left[k_p^2 + \frac{4(2\mu+\nu+1)}{r_0^2}\right]. \tag{6}$$

C. Co-propagation of multiple modes

An individual laser mode with a matched spot-size, which is a solution to Eq. (1), will propagate without intensity variation down a plasma channel. However, if one were to inject two or more overlapping Laguerre or Hermite-Gaussian modes into a plasma channel the modes would interfere and induce beating, affecting the wakefield. For modes a_1 and a_2 of arbitrary mode numbers, the intensity profile will have the following form:

$$\begin{aligned}|a|^2 &= |a_1 + a_2|^2 = (a_1 + a_2)(a_1^* + a_2^*) \\ &= |a_1|^2 + |a_2|^2 + a_1 a_2^* + a_1^* a_2.\end{aligned} \tag{7}$$

For linearly polarized, Hermite-Gaussian modes,

$$k_{\mathrm{beat},H} z = [(m_1 + n_1) - (m_2 + n_2)]z/Z_R. \tag{8}$$

For linearly polarized, Laguerre-Gaussian modes,

$$k_{\mathrm{beat},L} z = [(2\mu_1 + \nu_1) - (2\mu_2 + \nu_2)]z/Z_R. \tag{9}$$

If the sum of the mode numbers for each individual mode are not equal there will be a beating term with a characteristic wavelength of $\lambda_{\mathrm{beat}} = 2\pi/k_{\mathrm{beat}}$. However, if

$$m_1 + n_1 = m_2 + n_2 \tag{10}$$

for Hermite-Gaussian modes, or

$$2\mu_1 + \nu_1 = 2\mu_2 + \nu_2 \tag{11}$$

for Laguerre-Gaussian modes, there will be no beating.

An example of this can be seen in Figure 1 for the Laguerre-Gaussian basis. Here we have plotted several examples of co-propagating modes in a matched parabolic channel. The base line in black is the double Gaussian pulse, the trivial result. We can see that when we propagate pairs of modes with different indices there will be oscillations in the on-axis intensity. Likewise, a greater difference between indices results in a higher frequency oscillation, e.g., $L_{20}+L_{00}$ vs. $L_{10}+L_{00}$. However,

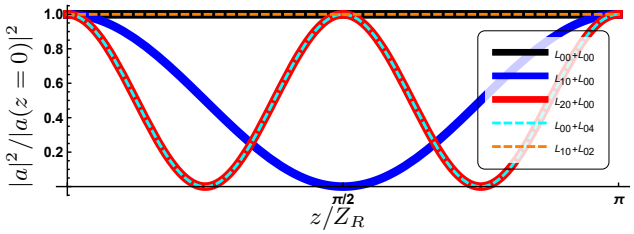

FIG. 1. Comparison of the on-axis intensity of co-propagating modes. The black line corresponds to two Gaussian modes, blue line to a_{10} and a_{00}, red line to a_{20} and a_{00}, dashed cyan line to a_{00} and a_{04}, and dashed orange line to a_{10} and a_{02}.

if we pick the indices such that the sum of the mode numbers is equal, according to Eqs. (10) and (11), we obtain matched propagation and no oscillations, e.g., for $L_{10} + L_{02}$.

In addition to the phase velocity we can derive an expression for the group velocity of a propagating mode. The general expression for the group velocity of a laser mode can be written as, $v_g/c = \partial\omega/\partial k$. For Hermite-Gaussian modes with matched spot size we have:

$$\frac{v_{g,H}}{c} = 1 - \frac{1}{2k^2}\left[k_p^2 + \frac{4(m+n+1)}{r_0^2}\right]. \tag{12}$$

For Laguerre-Gaussian modes with matched spot size we have:

$$\frac{v_{g,L}}{c} = 1 - \frac{1}{2k^2}\left[k_p^2 + \frac{4(2\mu+\nu+1)}{r_0^2}\right]. \tag{13}$$

This demonstrates the standard result that light propagates at a group velocity slower than the speed of light while traversing through a medium, i.e., $v_g < c$. From this we can also note that a wave packet composed of higher-order modes propagates through a plasma more slowly than one composed of lower order modes.

III. GEOMETRIC TUNING OF THE WAKEFIELD

In the linear regime the response of the wake can be determined from the normalized electrostatic potential, $\phi = e\Phi/m_e c^2$, where Φ is the scalar potential, governed by the equation $(\partial^2/\partial\zeta^2 + k_p^2)\phi = k_p^2 a^2/2$. In terms of the comoving variable $\zeta = z - v_g t$, we have the Green's function solution:

$$\phi = \frac{k_p}{4}\int_\infty^\zeta d\zeta' \sin[k_p(\zeta - \zeta')]|\hat{a}(r,\zeta')|^2, \tag{14}$$

where $\hat{a}(r,\zeta) = a_\perp(r)g(\zeta)$, $g(\zeta) = \exp[-(\zeta-\zeta_0)^2/L^2]$ is the longitudinal profile of the laser pulse (assumed Gaussian) and ζ_0 is the laser centroid. Note that this formulation assumes that the group velocities of all the modes are approximately the same, e.g., $v_{g,H}(m=0,n=2) \approx v_{g,H}(m=2,n=0) \approx c$, which assumes the quasi-static

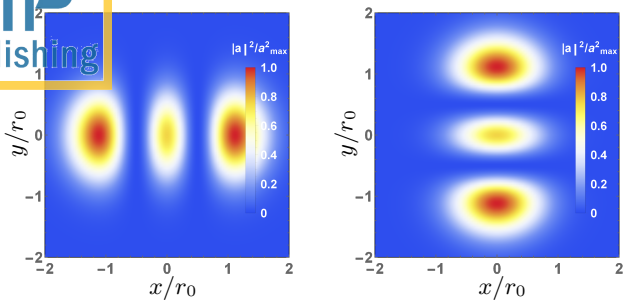

(a) (b)

FIG. 2. Comparison of $|a|^2$ for higher-order Hermite-Gaussian modes (a) $m_1 = 2, n_1 = 0$ and (b) $m_2 = 0, n_2 = 2$. Color denotes the amplitude intensity a^2.

approximation such that the laser evolves slowly with respect to the k_p^{-1}. The transverse electric field is given by

$$E_\perp/E_0 = -k_p^{-1}\nabla_\perp\phi. \tag{15}$$

We can use any number of modes to manipulate the wakefields, but in order to have a longitudinal accelerating field on-axis we need to choose modes that have an on-axis peak, i.e., in the Hermite-Gaussian basis, even number mode indices and in the Laguerre-Gaussian basis, radial modes. The lowest-order example of this mechanism that allows for independent control of the x and y components is the superposition of two Hermite-Gaussian modes, with $m_1 = 2, n_1 = 0$ and $m_2 = 0, n_2 = 2$. The intensity profiles of these two, independent modes can be seen in Figure 2.

The superposition of these modes can be controlled in several ways. The full expression of the intensity for these two modes is given by:

$$|a|^2 = \frac{1}{2}\left[a_{20}^2\left(1-4\frac{x^2}{r_0^2}\right)^2 + a_{02}^2\left(1-4\frac{y^2}{r_0^2}\right)^2 + 2a_{20}a_{02}\left(1-4\frac{x^2}{r_0^2}\right)\left(1-4\frac{y^2}{r_0^2}\right)\cos(\Delta\varphi)\right] \times e^{-2(x^2+y^2)/r_0^2}e^{-2(\zeta-\zeta_0)^2/L^2}, \tag{16}$$

where $\Delta\varphi$ is the difference between the initial phases of the two modes. The first concern is the initial, arbitrary phase factor that each mode brings to the intensity profile. The effect of an initial phase factor can be observed in Figure 3 and it can be deduced that the intensity is sensitive to the phase difference between the two modes, as a difference of $\Delta\varphi = \pi$ can extinguish the on-axis intensity peak (only if $a_{20} = a_{02}$).

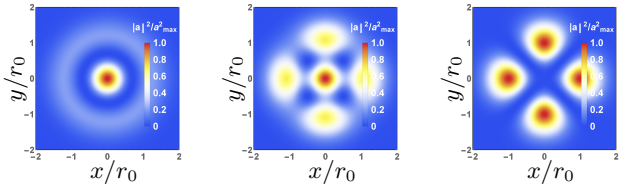

(a) (b) (c)

FIG. 3. Comparison of $|a|^2$ for the superposition of higher-order Hermite-Gaussian modes $m_1 = 2, n_1 = 0$ and $m_2 = 0, n_2 = 2$ with equal amplitudes $a_{20} = a_{02}$. (a) $\Delta\varphi = 0$, (b) $\Delta\varphi = \pi/2$, and (c) $\Delta\varphi = \pi$. Color denotes the amplitude intensity a^2.

A. Wakefield excited by $H_0H_2 + H_2H_0$ and $L_{10} + L_{02}$ laser modes

When considering a charged particle beam in the resonantly driven plasma wave behind the laser driver, $|\zeta - \zeta_0| \gg L$, where the laser amplitude is negligible, and when the phase difference is zero, i.e., $\Delta\varphi = 0$, the transverse electric fields derived from Eqs. (14), (15), and (16) can be written as:[22]

$$\frac{E_x}{E_0} = \sqrt{8\pi}\frac{xL}{r_0^2}\left[a_{20}\left(5-4\frac{x^2}{r_0^2}\right)+a_{02}\left(1-4\frac{y^2}{r_0^2}\right)\right] \times\left[a_{20}\left(1-4\frac{x^2}{r_0^2}\right)+a_{02}\left(1-4\frac{y^2}{r_0^2}\right)\right] \times e^{-k_p^2L^2/8}e^{-2(x^2+y^2)/r_0^2}\sin[k_p(\zeta-\zeta_0)], \tag{17}$$

$$\frac{E_y}{E_0} = \sqrt{8\pi}\frac{yL}{r_0^2}\left[a_{20}\left(1-4\frac{x^2}{r_0^2}\right)+a_{02}\left(5-4\frac{y^2}{r_0^2}\right)\right] \times\left[a_{20}\left(1-4\frac{x^2}{r_0^2}\right)+a_{02}\left(1-4\frac{y^2}{r_0^2}\right)\right] \times e^{-k_p^2L^2/8}e^{-2(x^2+y^2)/r_0^2}\sin[k_p(\zeta-\zeta_0)]. \tag{18}$$

Figure 4 portrays the intensity profile a^2, 4(a), 4(c), and 4(e), for two Hermite-Gaussian modes, and the corresponding transverse electric field, 4(b), 4(d), and 4(f), for three different instances of varying modal amplitude contributions. The arrows denote the direction of the electric field and the color its strength. Here we have two modes $m_1 = 2, n_1 = 0$ and $m_2 = 0, n_2 = 2$ with three different sets of coefficients: 4(a), 4(b) $a_{20} = a_{02} = 1$, 4(c), 4(d) $a_{20} = 1, a_{02} = 0.5$, and 4(e), 4(f) $a_{20} = -1, a_{02} = 5$. In 4(c) and 4(d) we can see a modest transverse asymmetry, while in 4(e) and 4(f) we see a strong asymmetry. Lineouts of the transverse x and y electric field can be seen in Figure 5. Considering the slopes of the x and y wakefields we can choose the relative value of the asymmetry using these two modes just as a function of the modal amplitude contributions, as has been depicted in Figure 6.

The same can be done with Laguerre-Gaussian modes, except following the matching condition $2\mu_1 + \nu_1 + 1 = 2\mu_2 + \nu_2 + 1$. An example of Laguerre-Gaussian mode matching can be seen in Fig. 7, where we plot the laser intensity and transverse electric field for a superposition of $\mu_1 = 1, \nu_1 = 0$ and $\mu_2 = 0, \nu_2 = 2$ modes. In this example we also have asymmetric focusing fields, with near-zero focusing along the y-axis and strong focusing along x-axis. These modes are phase matched so there will be no mode beating and both will propagate at the same group velocity.

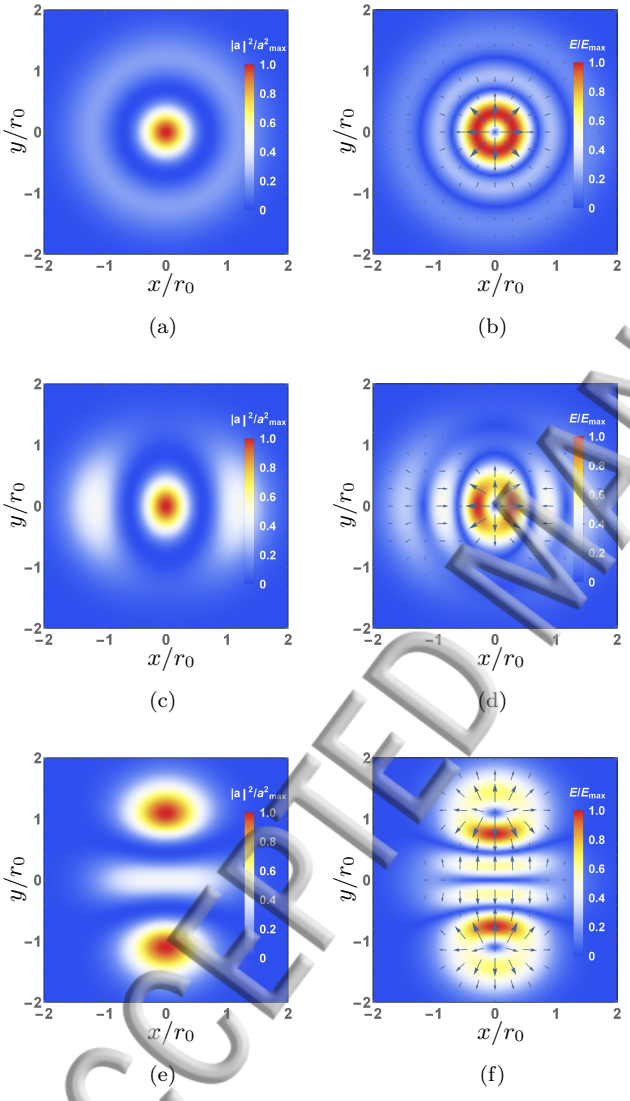

FIG. 4. Comparison of the superposition of higher-order Hermite-Gaussian modes $m_1 = 2, n_1 = 0$ and $m_2 = 0, n_2 = 2$ with respect to the laser intensity a^2 and the transverse electric field $E_\perp/E_0$. In subfigures (a) and (b) $a_{20} = a_{02} = 1$, (c) and (d) $a_{20} = 1$ and $a_{02} = 0.5$, and (e) and (f) $a_{20} = -1$ and $a_{02} = 5$. The color denotes the amplitude and field intensities and the arrows the transverse direction of the field.

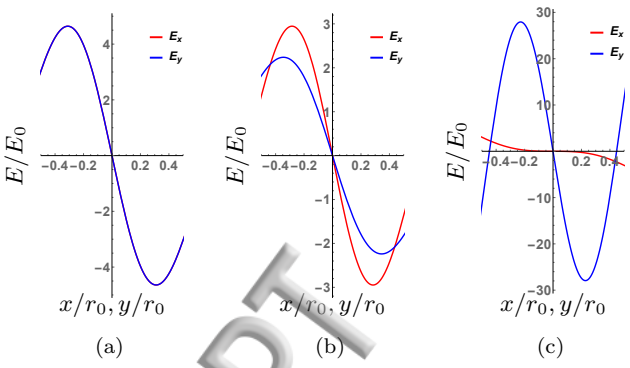

FIG. 5. Comparison of the superposition of higher-order Hermite-Gaussian modes $m_1 = 2, n_1 = 0$ and $m_2 = 0, n_2 = 2$ with respect to a lineout of the transverse electric field $E_\perp/E_0$. In subfigure (a) $a_{20} = a_{02} = 1$, (b) $a_{20} = 1$ and $a_{02} = 0.5$, and (c) $a_{20} = -1$ and $a_{02} = 5$.

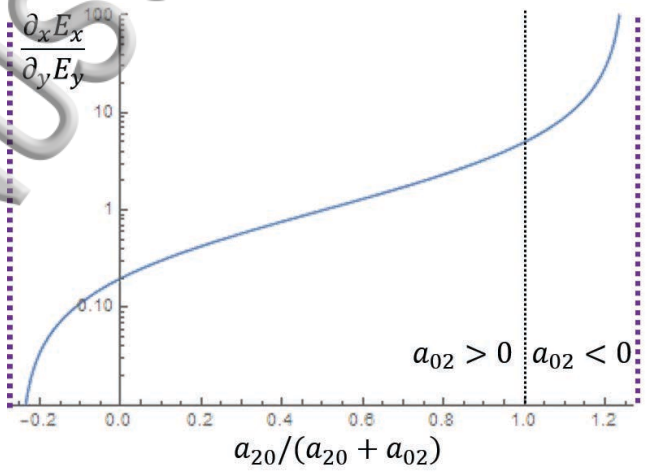

FIG. 6. Ratio of the slopes for $\partial_x E_x$ and $\partial_y E_y$ with constant longitudinal field E_z. There is freedom in picking the asymmetry of the wakefield just by modifying the amplitudes of the individual modes. For H_{20} and H_{02}, there are poles at $a_{20}/(a_{20} + a_{02}) = 1.25$ and -0.25.

B. Electron bunch propagation in an $H_0H_2 + H_2H_0$ wake

Near the axis, $x, y \ll r_0$, the regime where we expect the bunch to propagate, we can consider just the linear contribution of the field. In subsequent analysis modeling bunch propagation we only consider the phase when the transverse field is maximum and when the longitudinal accelerating field is near-zero, i.e., $k_p(\zeta - \zeta_0) = l\pi/2$, where l is an integer. The reason for this is to simplify our particle tracking and to clearly present the effects of higher-order modes. This analysis can readily be extended to a proper accelerating and focusing bucket of

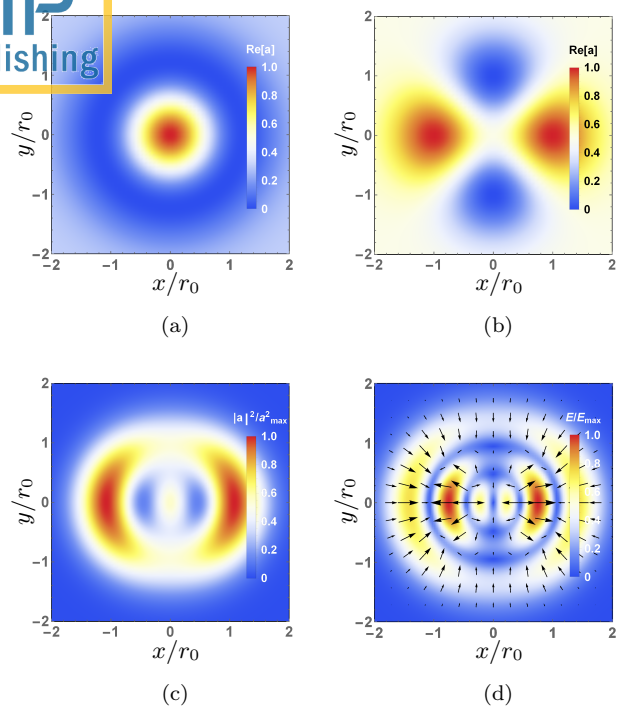

FIG. 7. Example of matched Laguerre-Gaussian modes L_{10} and L_{02} with $a_{10} = 1$ and $a_{02} = 3/2$. (a) the real component of mode L_{10}, (b) the real component of mode L_{02}, (c) the overall intensity profile $|a|^2 = |a_{10} + a_{02}|^2$, and (d) the corresponding transverse electric wakefield, where the color denotes the strength of the field and the arrows the direction.

the wake. The linear field can be expressed as

$$\frac{E_x}{E_0} \approx \sqrt{8\pi}\frac{L}{r_0^2} e^{-\frac{k_p^2 L^2}{8}} |(a_{02}+a_{20})(a_{02}+5a_{20})| x = -K_x^2 k_p x, \tag{19}$$

$$\frac{E_y}{E_0} \approx \sqrt{8\pi}\frac{L}{r_0^2} e^{-\frac{k_p^2 L^2}{8}} |(a_{02}+a_{20})(5a_{02}+a_{20})| y = -K_y^2 k_p y, \tag{20}$$

where $K_x^2 = \sqrt{8\pi}(L/r_0^2)\exp[-k_p^2L^2/8]|(a_{02} + a_{20})(a_{02} + 5a_{20})|$ and $K_y^2 = \sqrt{8\pi}(L/r_0^2)\exp[-k_p^2L^2/8]|(a_{02} + a_{20})(5a_{02} + a_{20})|$. From the linear fields we can compute the betatron frequency of a particle being focused by the wakefields:

$$\omega_{\beta x}^2 = K_x^2 \omega_p^2/\gamma \tag{21}$$

and similarly for $\omega_{\beta y}$, where $\gamma m_e c^2$ is the bunch energy.

We can numerically model a bunch propagating in such wakefields using a split-step, leapfrog integration scheme. The electron bunch spatial distribution is assumed to be Gaussian with σ_{x0}, σ_{y0} being respectively, the horizontal and vertical rms bunch spot sizes. In order to have matched propagation, the bunch momentum distribution is assumed to be Gaussian with an rms distribution $\sigma_{p_{x0}} = m_e c\gamma_0 k_\beta \sigma_{x_0}$ and likewise for $\sigma_{p_{y_0}}$, where $k_{\beta x} = \omega_{\beta x}/c$ and similarly for $k_{\beta y}$. If an electron bunch with these values is injected into a linear focusing field and there is no correlation term, i.e., $\langle xx' \rangle = 0$, there will be no betatron oscillations. The rms normalized emittance can be written as

$$\epsilon_x = \sqrt{\langle x^2\rangle\langle u_x^2\rangle - \langle x u_x\rangle^2}, \tag{22}$$

where $u_x = p_x/(m_e c)$. An analogous expansion exists for the $y-$direction. The angular brackets $\langle \ . \ \rangle$ represent an average over the bunch particle distribution. The rms emittance will be constant for linear focusing forces and for a mono-chromatic bunch.

All the wakefields are inherently non-linear and the use of higher-order modes further constrains the region of linearity near the axis. An example of this can be seen in Figure 8, where in 8(a) we have a bunch for which $\sigma_{x_0} = \sigma_{y_0} = 0.03r_0$ and in (b) we have $\sigma_{x_0} = \sigma_{y_0} = 0.1r_0$. Laser-plasma parameters are on-axis amplitude of $|a| = 0.1$, plasma density $n_0 = 3 \times 10^{17}$ cm^{-3}, and laser spot size $r_0 = 50$ μm. In Figure 8(b) we see emittance growth due to the bunch being wide enough to sample the nonlinear region of the wakefields. Due to this, using higher-order modes often requires the electron bunch to be tightly focused relative to the laser driver, with the bunch spot size being about 5% that of the laser driver or less.

We can demonstrate the potential for a matched, asymmetric laser driver when considering a situation in which we desire to guide a bunch with asymmetric emittances, e.g., the final focus in an accelerator. Considering a bunch with matched spot sizes, $\sigma_{x_0} = \sigma_{y_0} = 0.003r_0$, but with an emittance ratio of $\epsilon_x/\epsilon_y = 10$, we can demonstrate that higher-order modes can control the bunch. Initial parameters are an on-axis amplitude of $|a| = 0.1$, plasma density $n_0 = 3 \times 10^{17}$ cm^{-3}, and laser spotsize $r_0 = 50$ μm. Since the fields in the presence of the bunch are approximately linear in this case, there will be no emittance growth but the spot size will still evolve. In Figure 9(a), we inject a symmetric bunch into a matched wakefield of a laser driver composed of H_0H_2 and H_2H_0 modes. This gives the trivial solution of constant emittance $\epsilon_x = \epsilon_y = 0.01\mu$m and relatively constant spot size. If we increase the emittance ϵ_x by a factor of 10 by increasing σ_{p_x} by a factor of 10 we can see in Figure 9(b) how the bunch is matched in the y direction but not the x direction, such that $\epsilon_x = 0.1\mu$m and $\epsilon_y = 0.01\mu$m. A mismatched bunch will undergo betatron oscillations and particles would be lost from the wakefield. However, if we keep the asymmetric electron bunch but tune the amplitude coefficients of the laser driver, i.e., $a_{02} = 0.0235$ and $a_{20} = -0.1235$, which still gives an on axis amplitude of $|a| = 0.1$, we obtain the result shown in Figure 9(c), with a larger bunch spot size $\sigma_x = \sigma_y = 0.0115r_0$ giving us similar emittances as before of $\epsilon_x = 0.1\mu$m and $\epsilon_y = 0.01\mu$m. In this plot we see two distinct emittances but equal spot sizes.

This manuscript was accepted by Phys. Plasmas. Click here to see the version of record.

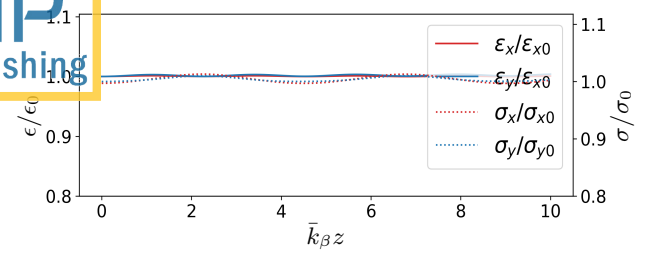

(a)

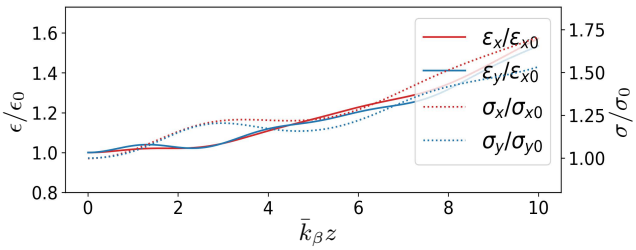

(b)

FIG. 8. Comparison of a bunch guided by the full, nonlinear wakefield of H_{02} and H_{20} modes for an initial bunch size of (a) $x_0 = 0.03r_0$ and (b) $x_0 = 0.1r_0$.

C. Potential limitations due to dephasing and efficiency

Two caveats of using higher-order modes are the effect of dephasing and the energy efficiency with respect to electron bunch acceleration. Dephasing between the accelerated electron bunch and the wake is a well known problem that is present in all LPA concepts. In the weakly-relativistic limit the dephasing limit for a higher-order mode in the Hermite-Gaussian basis can be approximated as

$$L_d \approx \frac{1}{2}\frac{\lambda_p^3}{\lambda^2}\left[1 + \frac{4(m+n+1)}{k_p^2 r_0^2}\right]^{-1}.$$

In current LPA systems a tapering of the background plasma density profile[23] along the path of acceleration is often proposed as one means to overcome dephasing as well as the implementation of multiple stages[24]. This is the same for higher-order laser modes, except given the fact that the group velocity is lower for higher-order modes than in the case for a Gaussian laser driver, the effective acceleration length would be reduced.

The issue of efficiency loss by the use of higher-order modes can be simply estimated by the ratio of the integrated laser intensity of the Gaussian mode, i.e., H_0H_0, relative to that of a superposition of higher-order modes, e.g., $H_2H_0 + H_0H_2$, assuming equal on-axis intensity, $a_{00}^2 = |a_{20} + a_{02}|^2$, i.e., for an equal accelerating gradient. For any two arbitrary, Hermite-Gaussian modes, this can be expressed as

$$\eta \propto \int_{-\infty}^{\infty}\int a_{00}^2 e^{-2\frac{(x^2+y^2)}{r_0^2}}dxdy \Big/ \int_{-\infty}^{\infty}\int \left|a_1 H_{m_1}\left(\frac{\sqrt{2}x}{r_0}\right)H_{n_1}\left(\frac{\sqrt{2}y}{r_0}\right) + a_2 H_{m_2}\left(\frac{\sqrt{2}x}{r_0}\right)H_{n_2}\left(\frac{\sqrt{2}y}{r_0}\right)\right|^2 e^{-2\frac{(x^2+y^2)}{r_0^2}}dxdy,$$

where we assume the same longitudinal profile for both profiles. For example, using the superposition of second-order modes as seen in Figure 4(a), where $a_{20} = a_{02} = 1$, would give us an effective efficiency loss of $\eta = 1/4$. However, if we want to guide or accelerate an electron bunch with an asymmetry ratio of $\epsilon_x/\epsilon_y = 10$ we need a laser profile as seen in Figure 4(c), which also approximately corresponds to the setup for particle tracking in Figure 9. This would lead to greater efficiency loss with $\eta \approx 1/13$. The relative increase in energy efficiency loss with respect to the Gaussian mode is intuitive as more energy content is located away from the axis.[25]

IV. FREQUENCY TUNING OF THE WAKEFIELD

In addition to geometric tuning there is also the freedom to select different frequencies for each of the independent modes. However, since the phase velocity is a function of the laser wavenumber k as well, it is not possible to select different, lower-order modes that propagate at the same group velocity and do not beat. This can be seen from the following expression,

$$|a|^2 = |a_1 + a_2|^2 = a_1^2 + a_2^2 + a_1 a_2 e^{i(k_1 z - v_{p,1}t)}e^{-i(k_2 z - v_{p,2}t)} + c.c.,$$

as having different wavenumbers to have equal v_p terms and thereby equal group velocities would result in a new beating contribution from the $(k_1 - k_2)z$ term. In order to prevent beating, one can either use two modes of orthogonal polarization or modes that are temporally separated and do not overlap, which are equivalent situations in terms of the interaction between the modes in the linear regime. Using orthogonal polarization limits one to only two modes in one instance as opposed to an indefinite number of arbitrary modes with temporal

This manuscript was accepted by Phys. Plasmas. Click here to see the version of record.

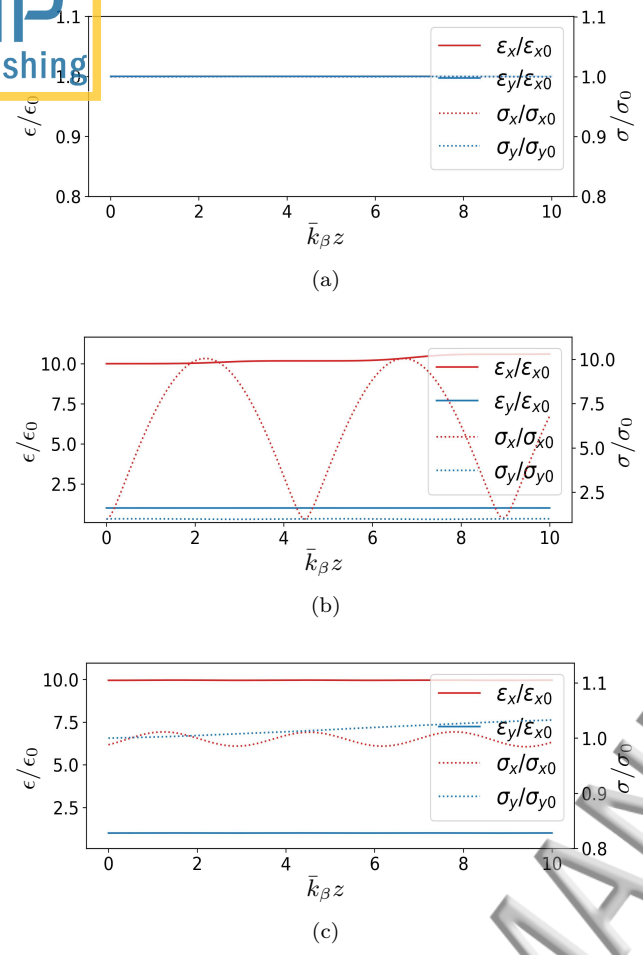

FIG. 9. Comparison of bunch guided by the fields of an H_{02} and H_{20} wake. (a) Initially matched bunch with $\epsilon_x/\epsilon_y = 1$ in a symmetric wake. (b) Initially mismatched bunch with $\epsilon_x/\epsilon_y = 10$ with matched bunch spot sizes in a symmetric wake. Due to the mismatch strong betatron oscillations can be observed. (c) Initially mismatched bunch with $\epsilon_x/\epsilon_y = 10$ with matched spot sizes in an asymmetric wake with coefficients $a_{02} = 0.0235$ and $a_{20} = -0.1235$.

separation. However, temporal separation may be more difficult to achieve experimentally, as each mode ought to be injected λ_p apart and would be more susceptible to longitudinal effects.

A. Wakefield excited by $L_{00} + L_{01}$ laser modes

For two Laguerre-Gaussian modes of indices $\mu_1 = \nu_1 = 0$ and $\mu_2 = 0, \nu_2 = 1$ and orthogonal polarization, the intensity profile can be written as:

$$|a|^2 = \frac{2}{\pi}\left(a_{00}^2 + 2\frac{r^2}{r_0^2}a_{01}^2\right)e^{-2r^2/r_0^2}e^{-2z^2/L^2}. \tag{23}$$

This is a superposition of the intensity profiles of a simple Gaussian and a first-order ring mode, as seen in Figure

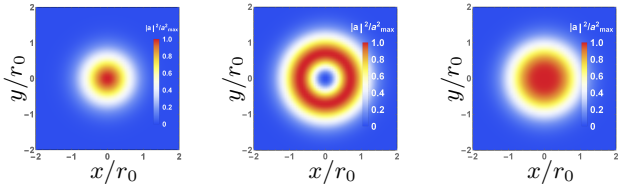

FIG. 10. Amplitude intensity profiles of Laguerre-Gaussian modes L_{00}, L_{01}, and their superposition $L_{00} + L_{10}$

10. In order for the two modes to co-propagate, it is necessary for them to have the same group velocity, and that can be done by solving for $k = \omega/c$ in Eq. (13). The general expression for matching the frequency of two Laguerre-Gaussian modes for co-propagation is,

$$\frac{1}{\lambda_2} = \frac{1}{\lambda_1}\sqrt{\frac{k_p^2 r_0^2 + 4(2\mu_2 + \nu_2 + 1)}{k_p^2 r_0^2 + 4(2\mu_1 + \nu_1 + 1)}}. \tag{24}$$

For example, in the case of an LPA system, with $n_0 = 3 \times 10^{17}$ cm^{-3}, $r_0 = 50$ μm, for $\lambda_{00} = 0.815$ μm we have $\lambda_{01} = 0.766$ μm.

When considering positions in the resonantly driven plasma wave far behind the laser driver, $|\zeta - \zeta_0| \gg L$ and orthogonal polarization, the transverse electric fields corresponding to Eqs. (14), (15), and (16) for L_{00} and L_{01} can be written as:

$$\frac{E_r}{E_0} = \sqrt{\frac{2}{\pi}}\frac{L}{r_0^2}\left[a_{00}^2 - a_{01}^2\left(1 - 2\frac{r^2}{r_0^2}\right)\right]e^{-k_p^2L^2/8} \times e^{-2r^2/r_0^2}\sin[k_p(\zeta - \zeta_0)]r, \tag{25}$$

$$\frac{E_z}{E_0} = \frac{k_pL}{\sqrt{8\pi}}\left(a_{00}^2 + 2a_{01}^2\frac{r^2}{r_0^2}\right)e^{-k_p^2L^2/8} \times e^{-2r^2/r_0^2}\cos[k_p(\zeta - \zeta_0)], \tag{26}$$

and the linear component of these fields, i.e., when $r/r_0 \ll 1$, can be written as:

$$\frac{E_r}{E_0} \approx \sqrt{\frac{2}{\pi}}\frac{L}{r_0^2}(a_{00}^2 - a_{01}^2)e^{-k_p^2L^2/8}\sin[k_p(\zeta - \zeta_0)]r, \tag{27}$$

$$\frac{E_z}{E_0} \approx \frac{k_pL}{\sqrt{8\pi}}a_{00}^2e^{-k_p^2L^2/8}\cos[k_p(\zeta - \zeta_0)]. \tag{28}$$

From the linear equations one can deduce that the longitudinal field depends primarily on the Gaussian mode and the higher-order mode L_{01} can independently modify the transverse fields. A lineout of the intensity profile and the corresponding transverse electric field can be seen in Figure 11. The thin solid lines correspond to just a Gaussian driver, the thick solid lines correspond to $a_{00} = a_{01}$ and to when the electric field is zero near the axis, while the dashed line corresponds to a modified Gaussian wake and the dot-dashed to a strongly modified wake.

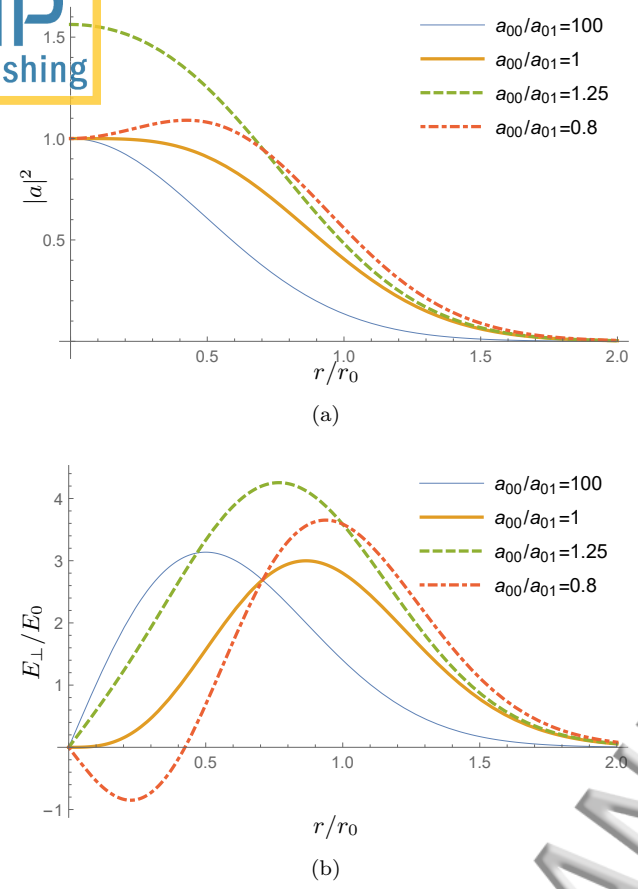

FIG. 11. Lineouts of the transverse profiles of Laguerre-Gaussian modes L_{00} and L_{01} for (a) the amplitude intensity $|a|^2$ and (b) for the transverse electric field $E_\perp/E_0$. The thin line is for $a_{00}/a_{01} = 100$, effectively just the Gaussian, the solid line is for $a_{00}/a_{01} = 1$, dashed for $a_{00}/a_{01} = 1.25$, and dot-dashed for $a_{00}/a_{01} = 0.8$.

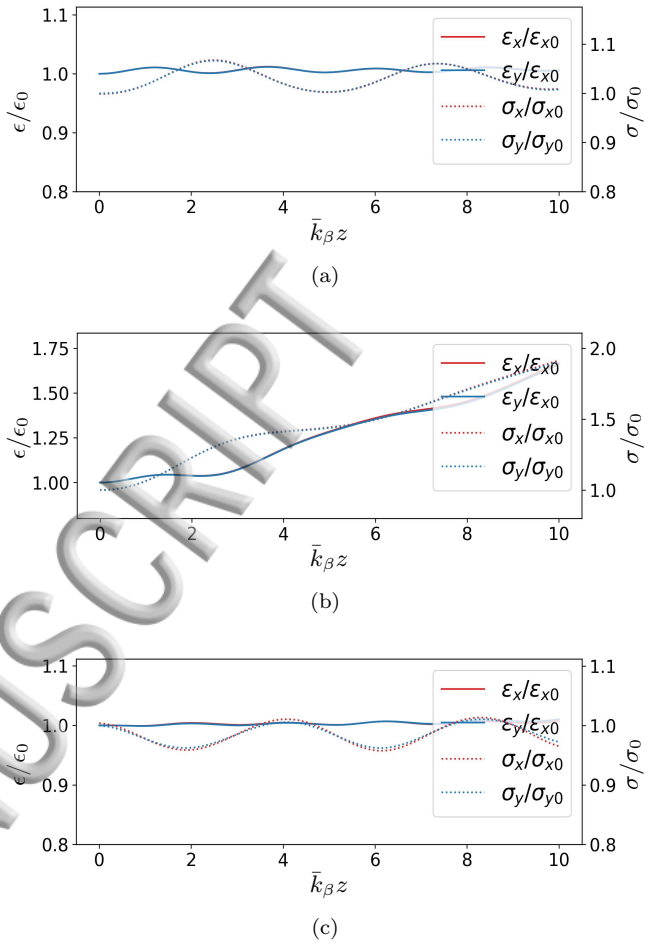

FIG. 12. Comparison of a bunch guided by the non-linear wakefields of an L_{00} and L_{01} laser driver. (a) Initially matched bunch with $\sigma_x = \sigma_y = 0.1r_0$ in a symmetric wake with $a_{00} = 0.1$ and $a_{01} = 0$. (b) Initially matched bunch with $\sigma_x = \sigma_y = 0.2r_0$ in a symmetric wake with $a_{00} = 0.1$ and $a_{01} = 0$. The bunch sees the non-linear field and emittance grows (c) Initially matched bunch with $\sigma_x = \sigma_y = 0.2r_0$ in a symmetric wake with $a_{00} = 0.1$ and $a_{01} = 0.08$. The softening of the transverse gradients reduces the experience of non-linear fields by the bunch and emittance remains effectively constant.

B. Bunch propagation in an $L_{00} + L_{01}$ wake

By using two modes we can tailor the focusing forces of the wakefields. Considering a bunch with emittance ratio $\epsilon_x/\epsilon_y = 1$ and propagating in the full, non-linear wakefields, we demonstrate that higher-order modes can be used to mollify the transverse fields and ensure matched propagation. Initial parameters are an on-axis amplitude of $|a| = 0.1$, plasma density $n_0 = 3 \times 10^{17}$ cm^{-3}, and laser spotsize $r_0 = 50$ μm. Likewise, we are only considering the focusing forces in this simulation, so $k_p(\zeta - \zeta_0) = l\pi/2$, where l is an integer. Numerical results can be found in Figure 12.

In Figure 12(a) we have an electron bunch with matched spot sizes, $\sigma_x = \sigma_y = 0.1r_0$ in the wake of a Gaussian pulse, i.e., L_{00} mode. This is the trivial result with constant emittance $\epsilon_x = \epsilon_y = 1.3$ μm and relatively constant spotsize. In Figure 12(b) we have a wider bunch with $\sigma_x = \sigma_y = 0.2r_0$ and the bunch begins to experience the non-linear contributions of the field and both emittance, initially $\epsilon_x = \epsilon_y = 5.3$ μm, and spot size grow. Keeping $a_0 = 0.1$, we introduce an L_{01} mode with amplitude $a_{01} = 0.08$ such that $a_{00}/a_{01} = 1.25$, which corresponds to the dashed lines in Figure 11. In this case we still have the wider, initial bunch spot size $\sigma_x = \sigma_y = 0.2r_0$ but relatively constant emittance $\epsilon_x = \epsilon_y = 3.2$ μm and spot size evolution, shown in Figure 12(c). Just as in the case for geometric tuning, frequency tuning is also physically limited by issues of dephasing and energy efficiency loss.

V. SUMMARY AND CONCLUSIONS

In this paper we propose the use of higher-order laser modes to modify and control the wakefields behind a laser driver. It was shown that modes of different geometric indices propagate at different group velocities and when co-propagating lead to mode beating. Using both the Hermite and Laguerre-Gaussian basis we demonstrated that, by choosing appropriate geometric indices, one would have a transverse mode structure that is non-Gaussian but does not beat and has all modes propagating at the same group velocity, (e.g., $H_2H_0 + H_0H_2$ and $L_{10} + L_{02}$). This can be used to create an asymmetric wake structure and allow for the focusing of asymmetric electron bunches with asymmetric transverse emittances, such as an emittance ratio of $\epsilon_x/\epsilon_y = 10$, which opens the possibility of using a laser-plasma lens structure as a final focus for a linear accelerator.

Likewise, we showed that one can also choose modes of different colors to allow for a wake with more complex structures but not limited by group velocity dispersion. However, these modes still beat and so they must be either of orthogonal polarizations or temporally separated. We showed that a pulse could be composed of two modes, $L_{00} + L_{01}$, and that we could vary the amplitude and thereby reducing the transverse gradients of the wakefield, allowing for the focusing of wider bunches. This is particularly relevant for positron beam acceleration and/or to avoid ion motion.

Experimental implementation of our theoretical results presupposes several conditions. One must have good control of the phase and polarization of the individual laser modes. It is shown that multimode pulses are sensitive to the phase content of the individual modes. In addition, one must be able to carefully and precisely generate the modes one wishes to use. Hermite-Gaussian modes can be generated using an off-axis pumping scheme.[26] For Laguerre-Gaussian modes, a spiral phase plate can be used to induce a helical phasefront in an injected laser beam.[27] Once the modes have been generated precise aiming and timing of the individual modes in addition to a combining optic in order to generate the desired multimode pulse. In order to also consider color tuning, one must be able to vary the frequency of a mode precisely. From a physical perspective, dephasing and efficiency loss are limitations to the proposed concept, but these can be addressed via density tapering and energy recover.

Advancements in laser technology have greatly spurred on LPA science and promise more possibilities in the future. While historically it has been sufficient to have a near Gaussian profile for the driver, further advances will require greater control and quality. Applying current techniques for the generation of higher-order laser modes to high-intensity, ultrashort laser pulse systems will be challenging, but the potential benefits of using the discussed mechanisms will greatly expand the potential for future LPA applications.

VI. ACKNOWLEDGMENTS

The authors acknowledge contributions from members of the BELLA Program at Lawrence Berkeley National Laboratory. This work was supported by the Director, Office of Science, Office of High Energy Physics, of the U.S. Department of Energy under Contract No. DE-AC02-05CH11231 as well as by the NSF through Grant No. PHY-1632796.

[1] T. Tajima and J.M. Dawson. *Phys. Rev. Lett.*, 43, 1979.
[2] E. Esarey, C.B. Schroeder, and W.P. Leemans. *Rev. Mod. Phys.*, 81:1229, 2009.
[3] W.P. Leemans and E. Esarey. *Phys. Today*, 62, 2009.
[4] C.B. Schroeder, E. Esarey, C.G.R. Geddes, C. Benedetti, and W.P. Leemans. *Phys. Rev. ST Accel. Beams*, 13, 2010.
[5] Z. Huang, Y. Ding, , and C.B. Schroeder. *Phys. Rev. Lett.*, 109, 2012.
[6] W.P. Leemans, A.J. Gonsalves, H.-S. Mao, K. Nakamura, C. Benedetti, C.B. Schroeder, Cs. Toth, J. Daniels, D.E. Mittelberger, S.S. Bulanov, J.-L. Vay, C.G.R Geddes, and E. Esarey. *Phys. Rev. Lett.*, 113:245002, 2014.
[7] B.Z. Djordjević, C. Benedetti, C.B. Schroeder, E. Esarey, and W.P. Leemans. *Phys. Plasmas*, 25:013103, 2018.
[8] S.G. Rykovanov, J.W. Wang, V.Yu. Kharin, B. Lei, C. B. Schroeder, C. G. R. Geddes, E. Esarey, and W. P. Leemans. *Phys. Rev. Acc. and Beams*, 19:090703, 2016.
[9] S.G. Rykovanov, C. B. Schroeder, C. G. R. Geddes, E. Esarey, and W. P. Leemans. *Phys. Rev. Lett.*, 114, 2015.
[10] J.W. Wang, C. B. Schroeder, R. Li, M. Zepf, and S.G. Rykovanov. *Sci. Rep.*, 7, 2017.
[11] J. Vieira, R.M.G.M. Trines, E.P. Alves, R.A. Fonseca, J.T. Mendonça, R. Bingham, P. Norreys, and L.O. Silva. *Phys. Rev. Lett.*, 117, 2017.
[12] J. Vieira and J. T. Mendonça. *Phys. Rev. Lett.*, 112, 2014.
[13] Guo-Bo Zhang, Min Chen, Ji Luo, Ming Zeng, Tao Yuan, Ji-Ye Yu, Yan-Yun Ma, Tong-Pu Yu, Lu-Le Yu, Su-Ming Weng, , and Zheng-Ming Sheng. *Jour. App. Phys.*, 119, 2016.
[14] E. Cormier-Michel, E. Esarey, C. G. R. Geddes, C. B. Schroeder, K. Paul, P. J. Mullowney, J. R. Cary, and W. P. Leemans. *Phys. Rev. Acc. and Beams*, 14:031303, 2011.
[15] E. Esarey, B.A. Shadwick, P. Catravas, and W.P. Leemans. *Phys. Rev. E*, 65, 2002.
[16] J.B. Rosenzweig, A.M. Cook, A. Scott, M.C. Thompson, and R.B. Yoder. *Phys. Rev. Lett.*, 95, 2005.
[17] C. Benedetti, C.B. Schroeder, E. Esarey, and W.P. Leemans. *Phys. Rev. Acc. and Beams.*, 20, 2017.
[18] L.-L. Yu, C.B. Schroeder, F.-Y. Li, C. Benedetti, M. Chen, S.-M. Weng, Z.-M. Sheng, and E. Esarey. *Phys. Plasmas*, 21, 2014.
[19] A.W. Chao, K.H. Mess, M. Tigner, and F. Zimmermann. *Handbook of Accelerator Physics and Engineering*. World Scientific Publishing Company, Singapore, 2013.
[20] C. Benedetti, F.Rossi, C.B. Schroeder, E.Esarey, and W.P. Leemans. *Phys. Rev. E*, 92:023109, 2015.
[21] E. Esarey, P. Sprangle, M. Pilloff, and J. Krall. *J. Opt. Soc. Am. B*, 12, 1995.
[22] L.M. Gorbunov and V.I. Kirsanov. *Zh. Eksp. Teor. Fiz.*, 93, 1986.
[23] W. Rittershofer, C. B. Schroeder, E. Esarey, F. J. Gr'uner, and W. P. Leemans. *Phys. Plasmas*, 17:063104, 2010.
[24] S. Steinke, J. van Tilborg, C. Benedetti, C. G. R. Geddes, C. B. Schroeder, J. Daniels, K. K. Swanson, A. J. Gonsalves, K. Nakamura, N. H. Matlis, B. H. Shaw, E. Esarey, and W. P. Leemans. *Nature*, 530:190–193, 2010.
[25] C. B. Schroeder, E. Esarey, C. Benedetti, and W. P. Leemans. *AIP Conf. Proc.*, 1777:020001, 2016.
[26] S.-C. Chu, Y.-T. Chen, K.-F. Tsai, and K. Otsuka. *Opt. Express*, 20, 2012.

[27] G.A. Turnbull, D.A. Robertson, G.M. Smith, L. Allen, and M.J. Padgett, *Opt. Commun.*, 127, 1996.

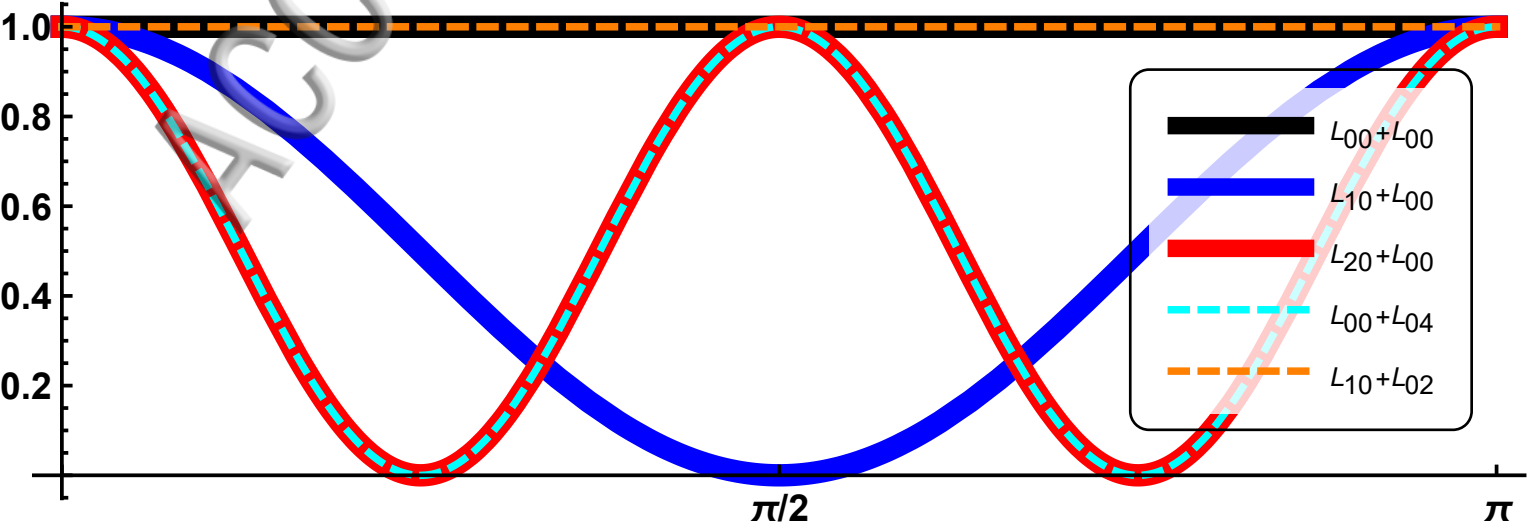
1.0
0.8
0.6
0.4
0.2
π/2
π
$L_{00}+L_{00}$
$L_{10}+L_{00}$
$L_{20}+L_{00}$
$L_{00}+L_{04}$
$L_{10}+L_{02}$

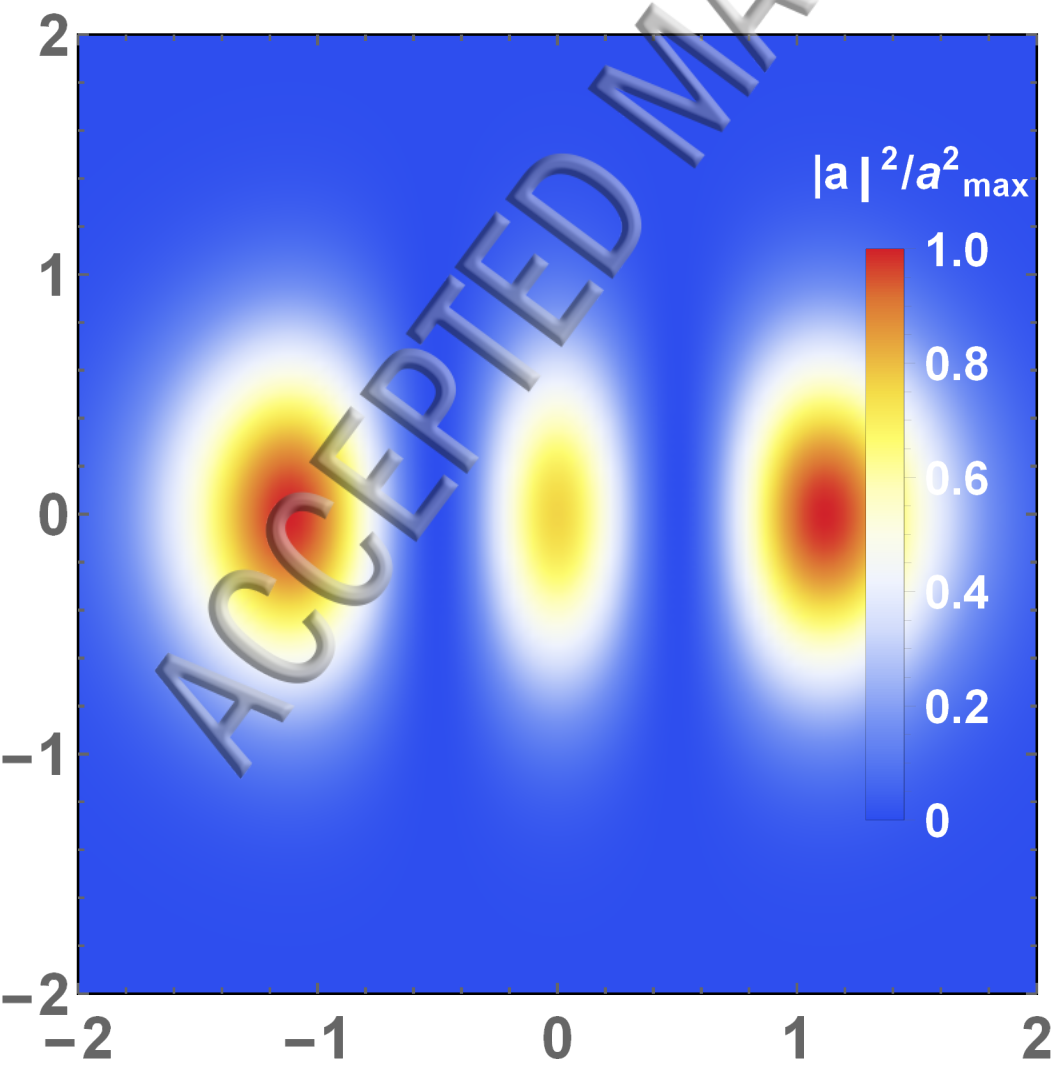

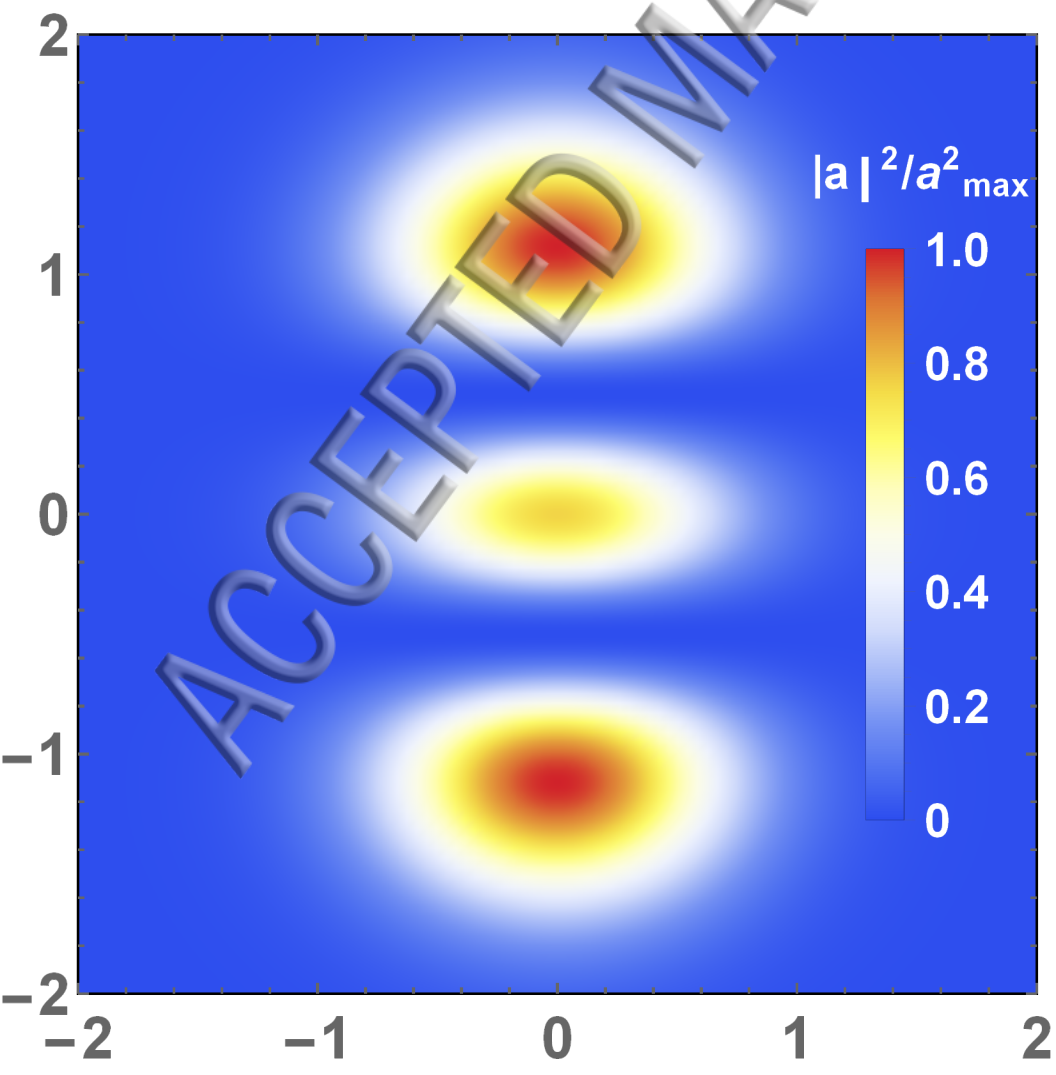

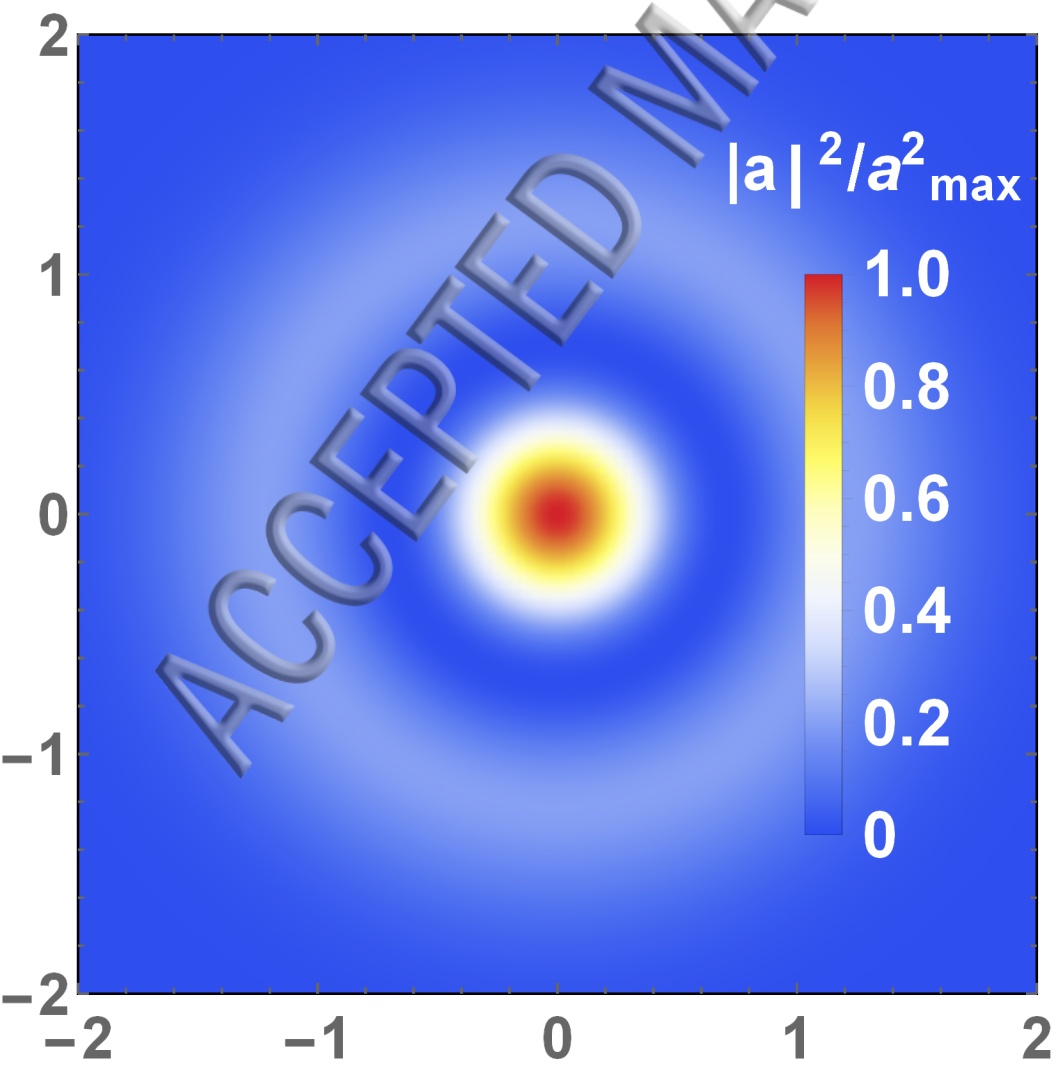

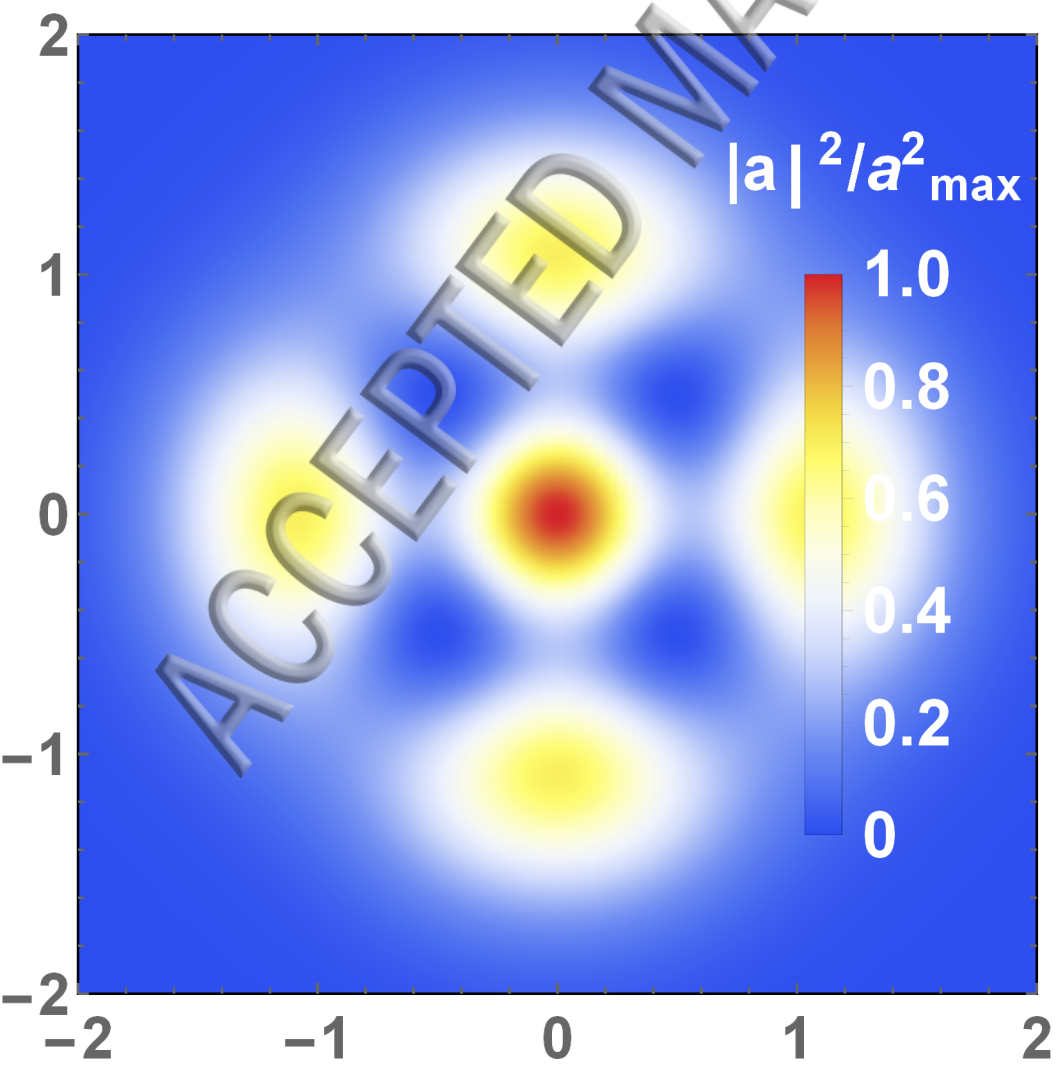

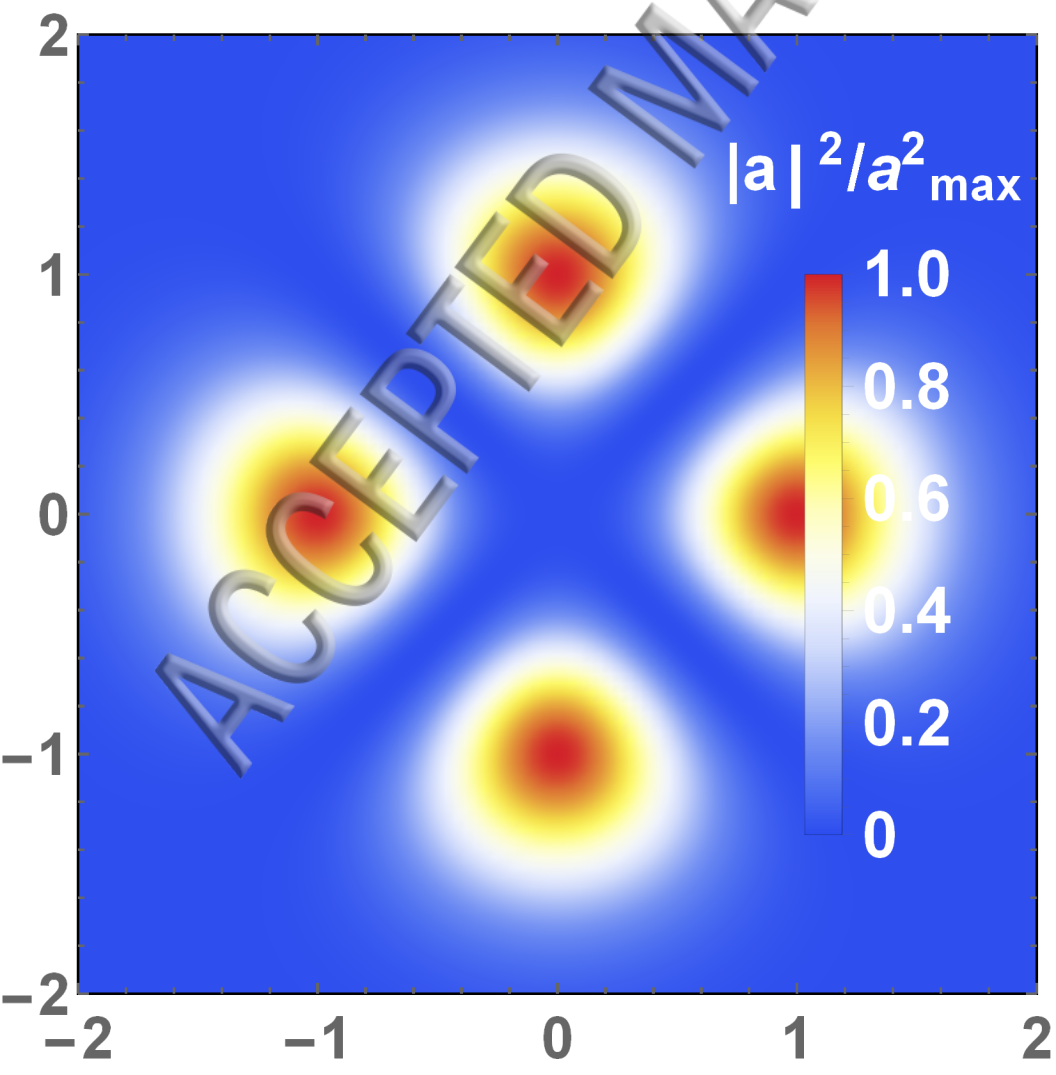

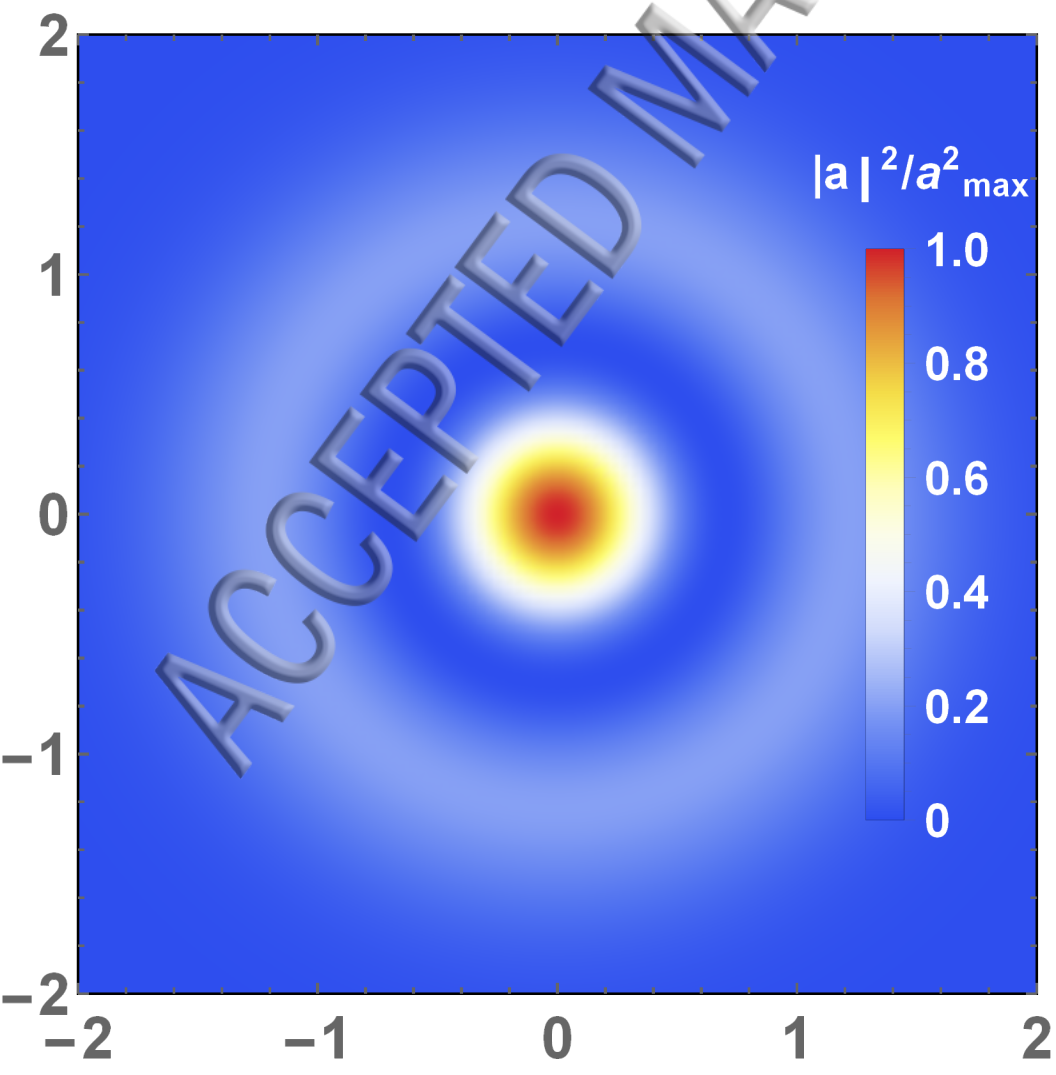

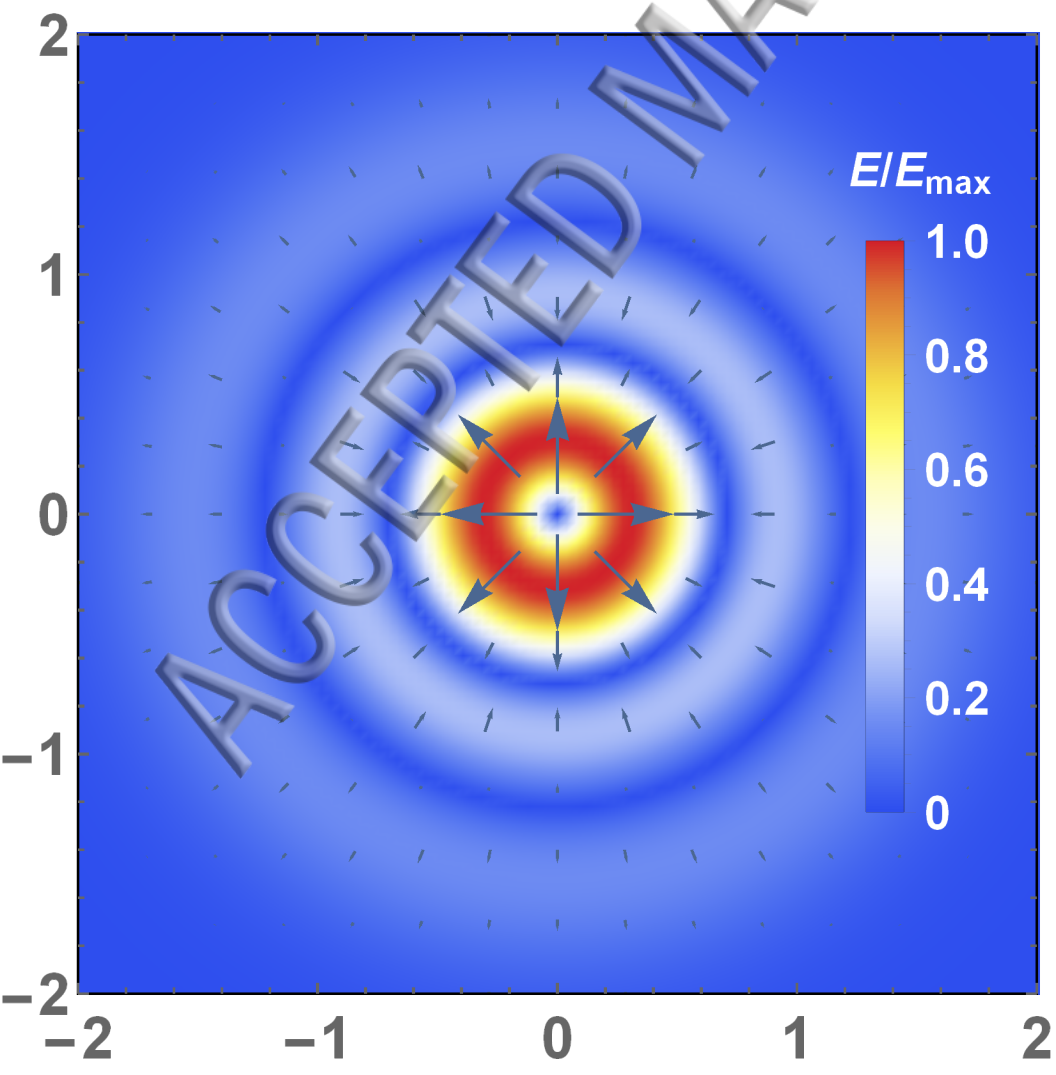

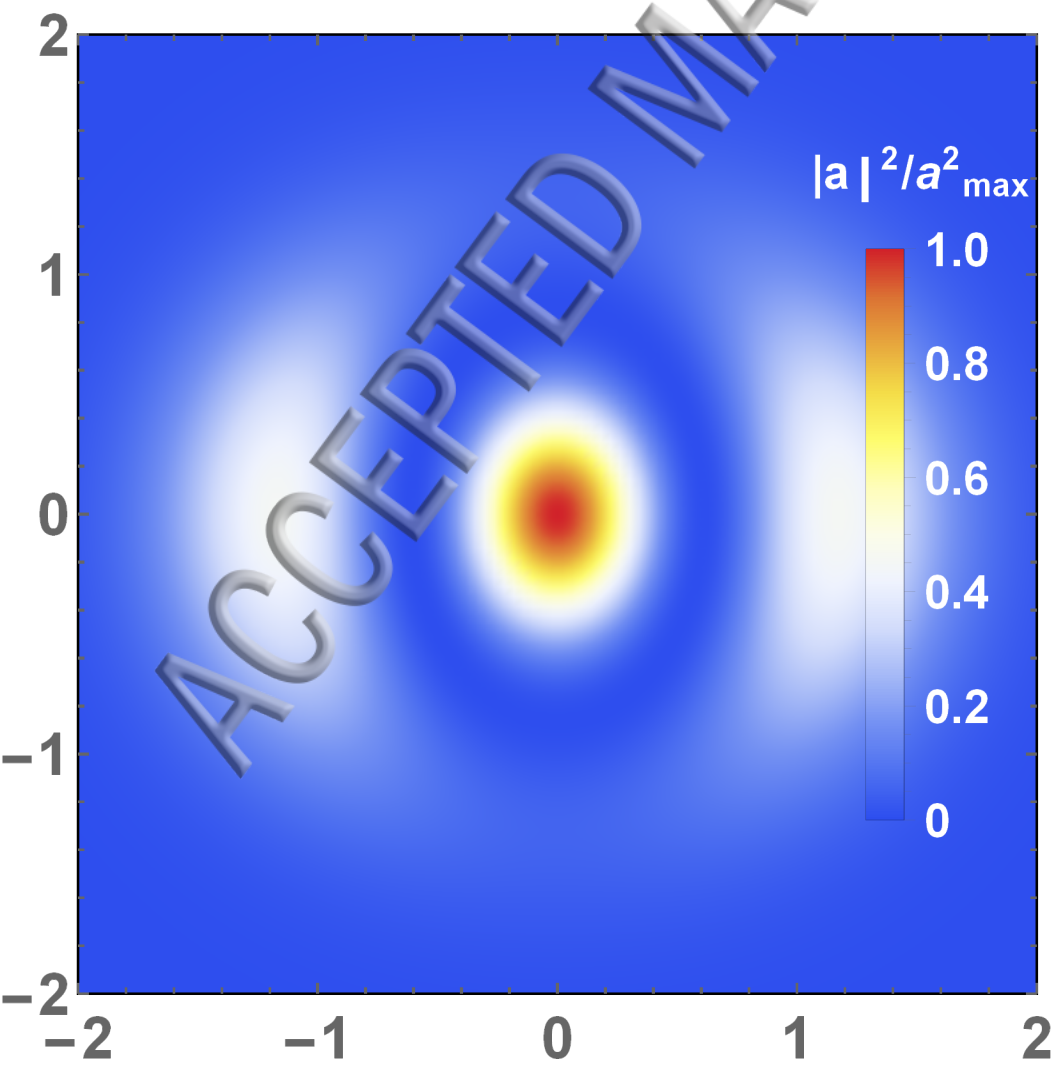

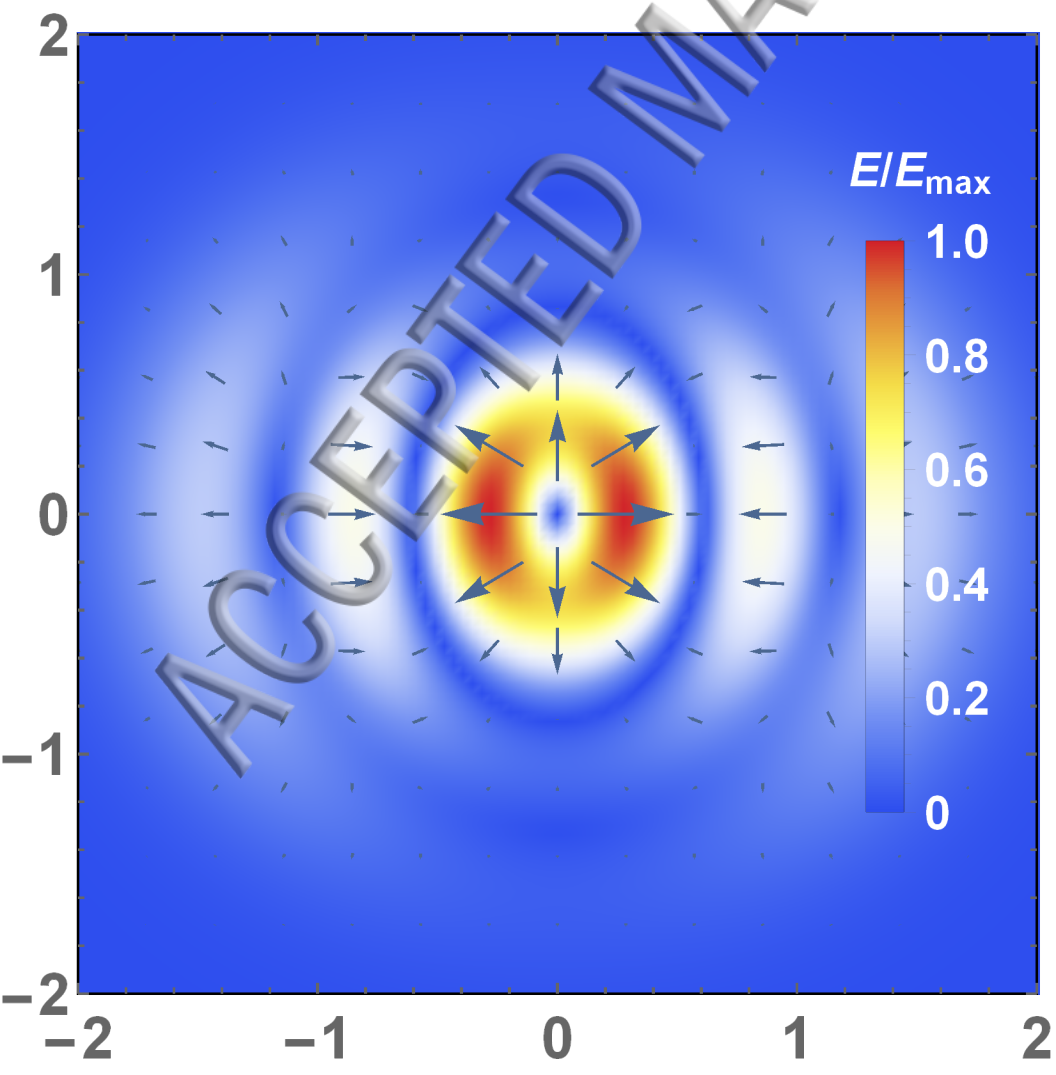

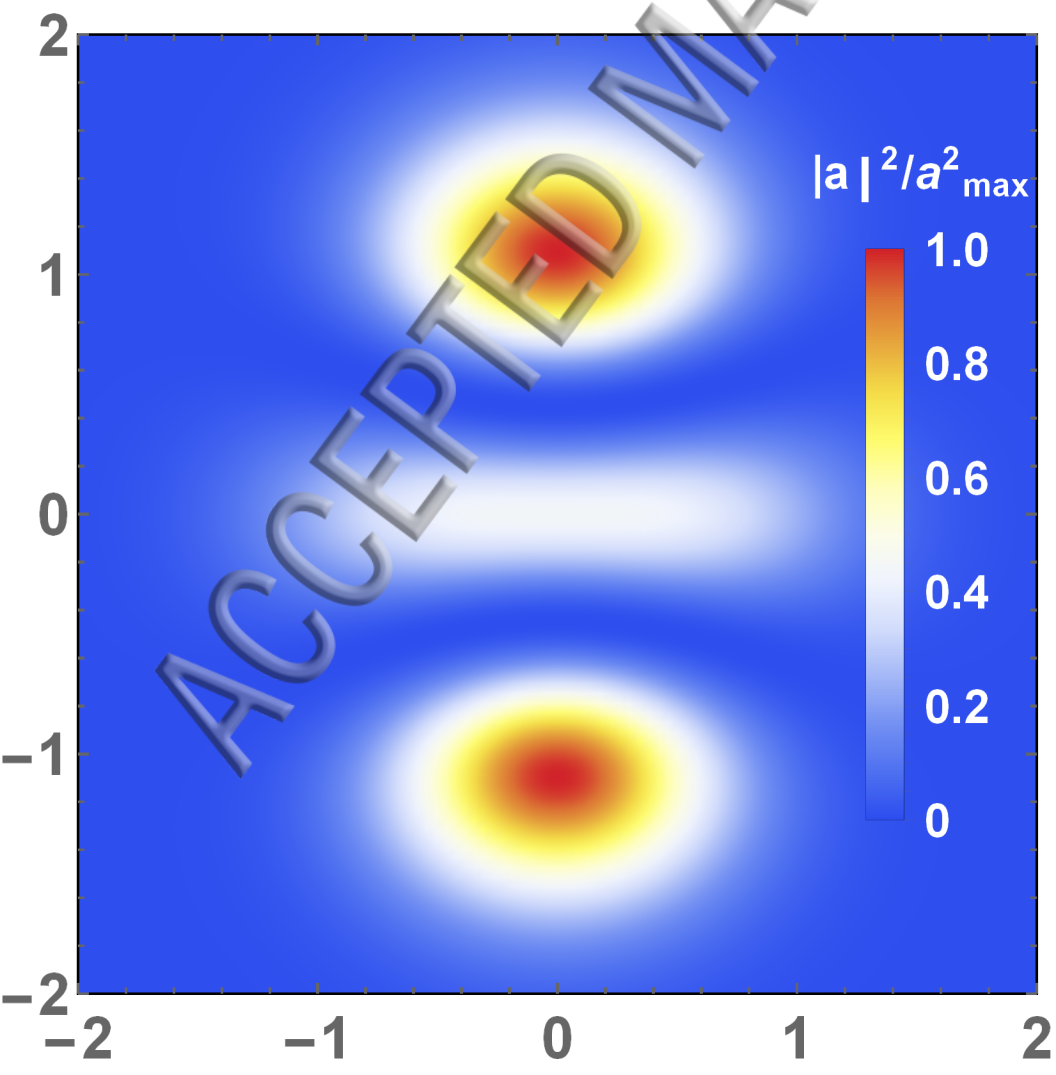

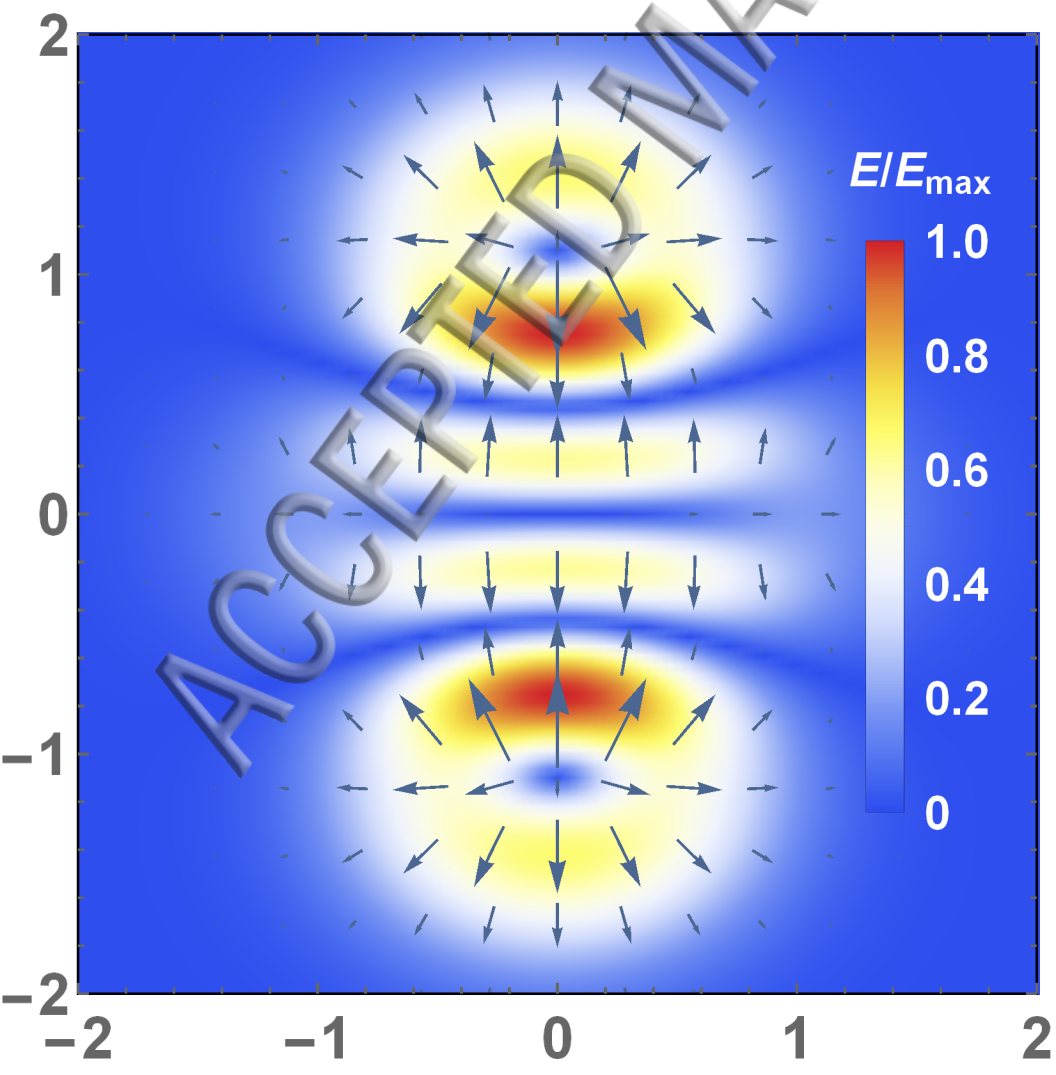

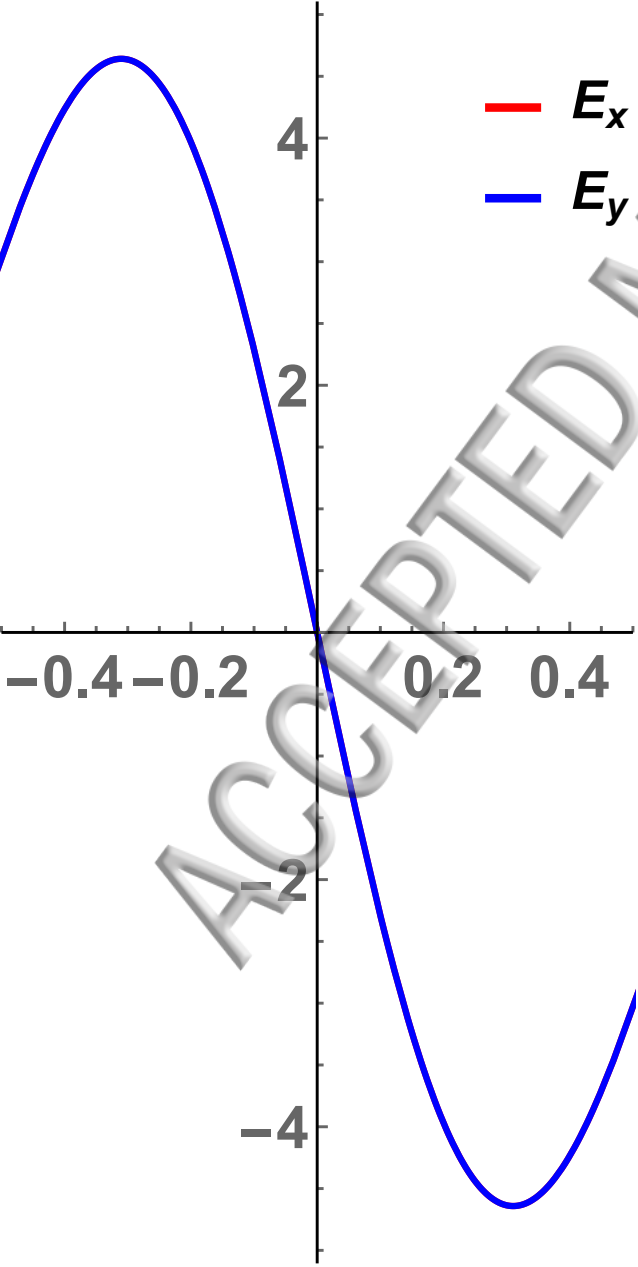

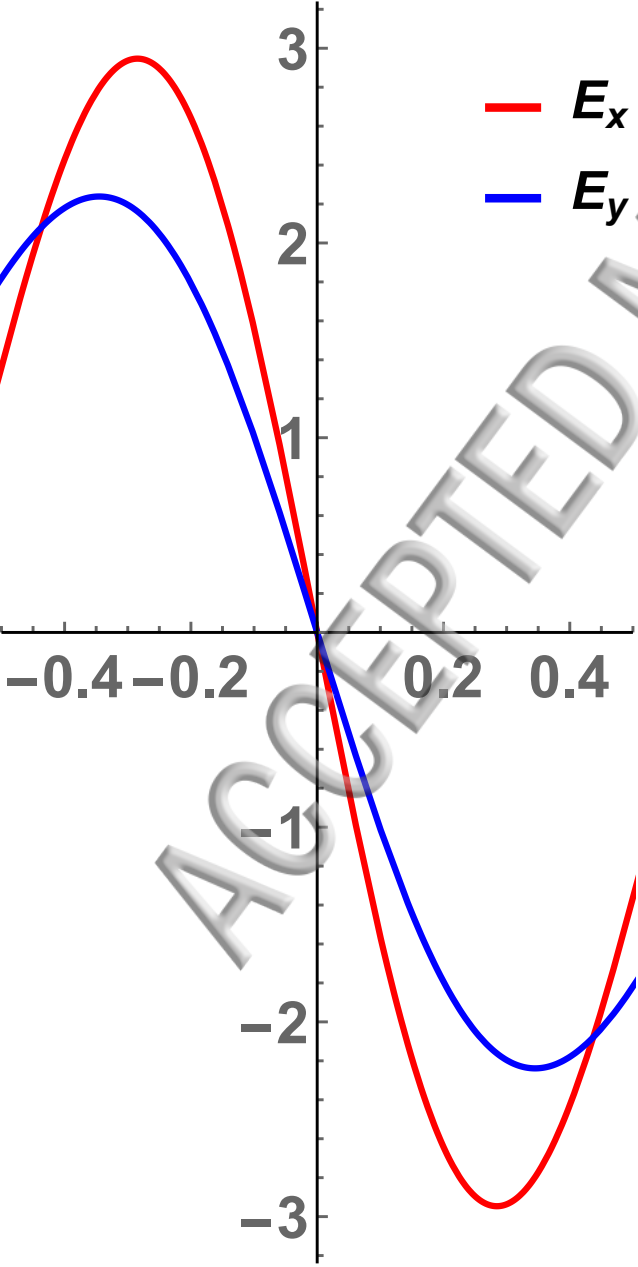

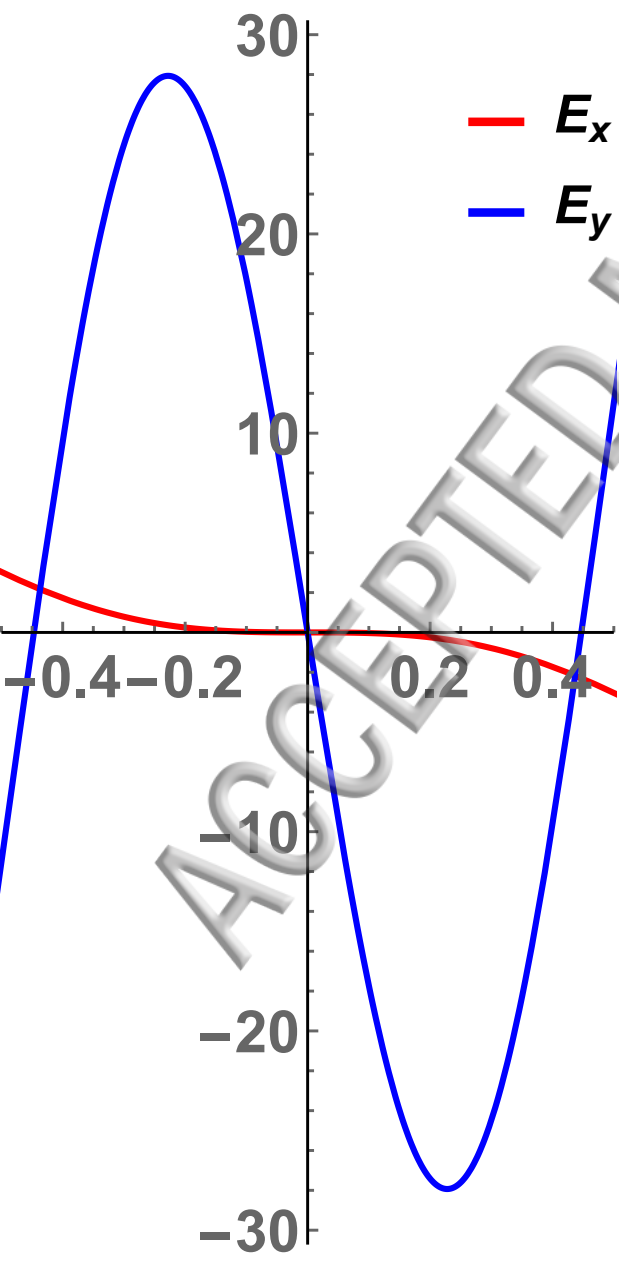

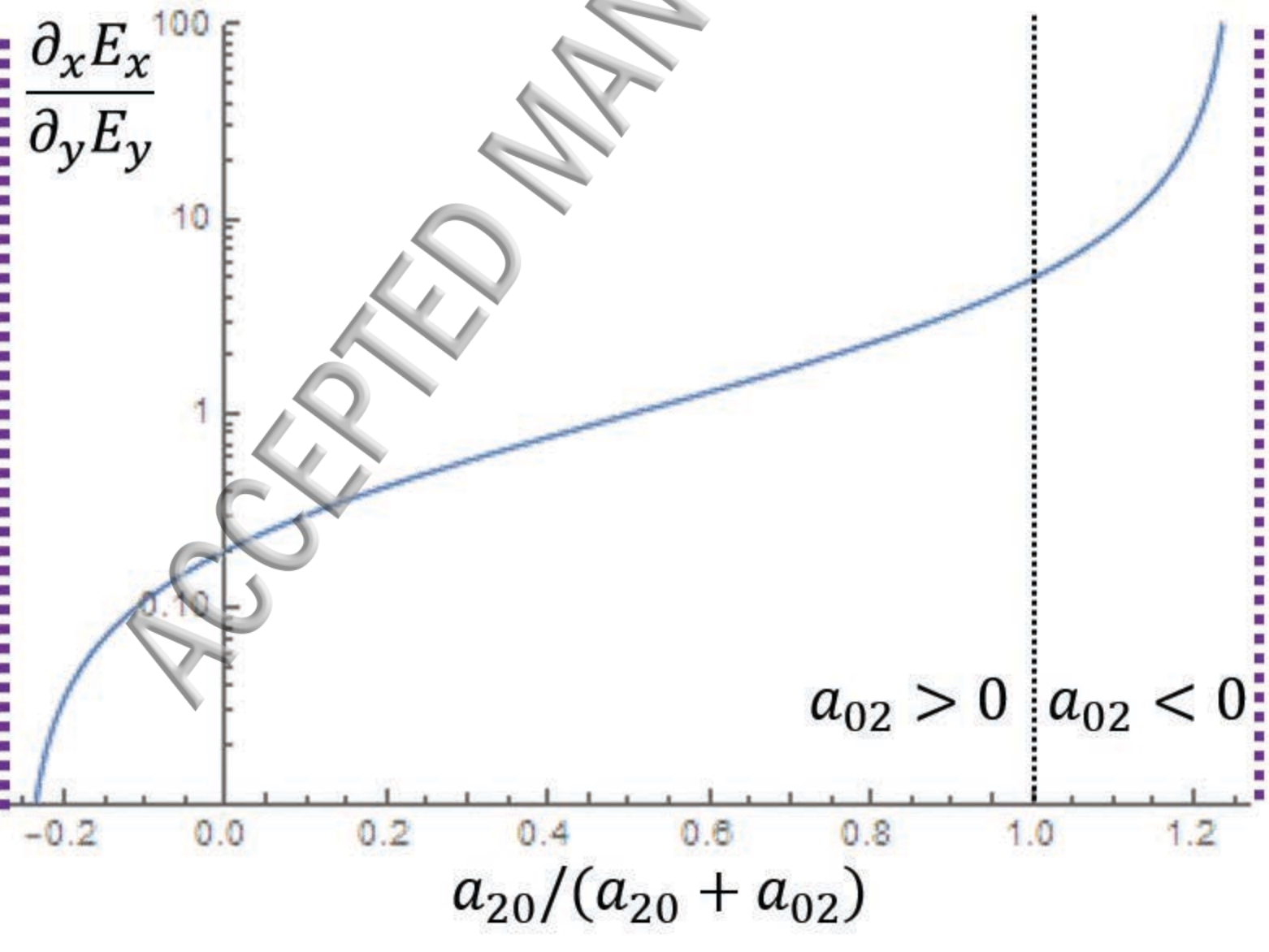

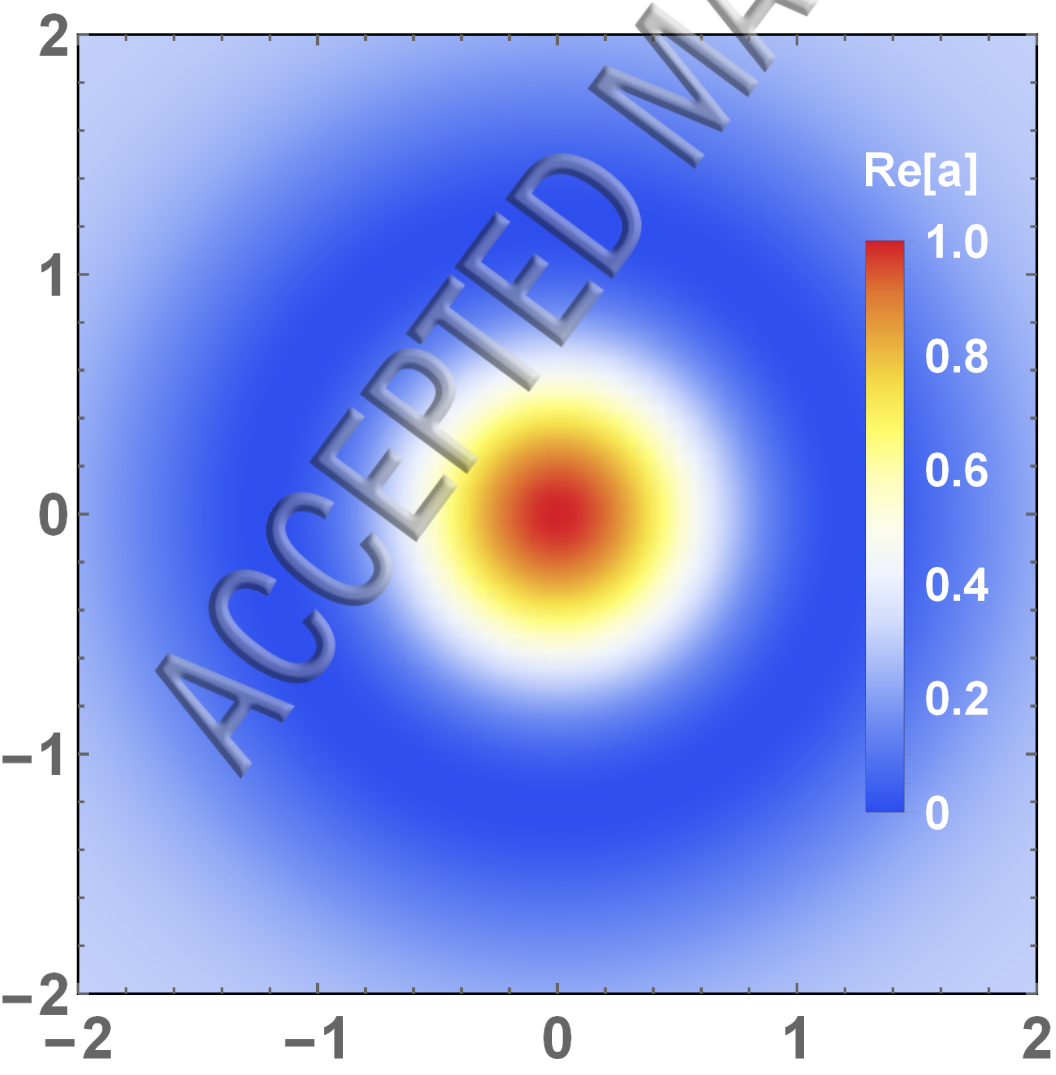

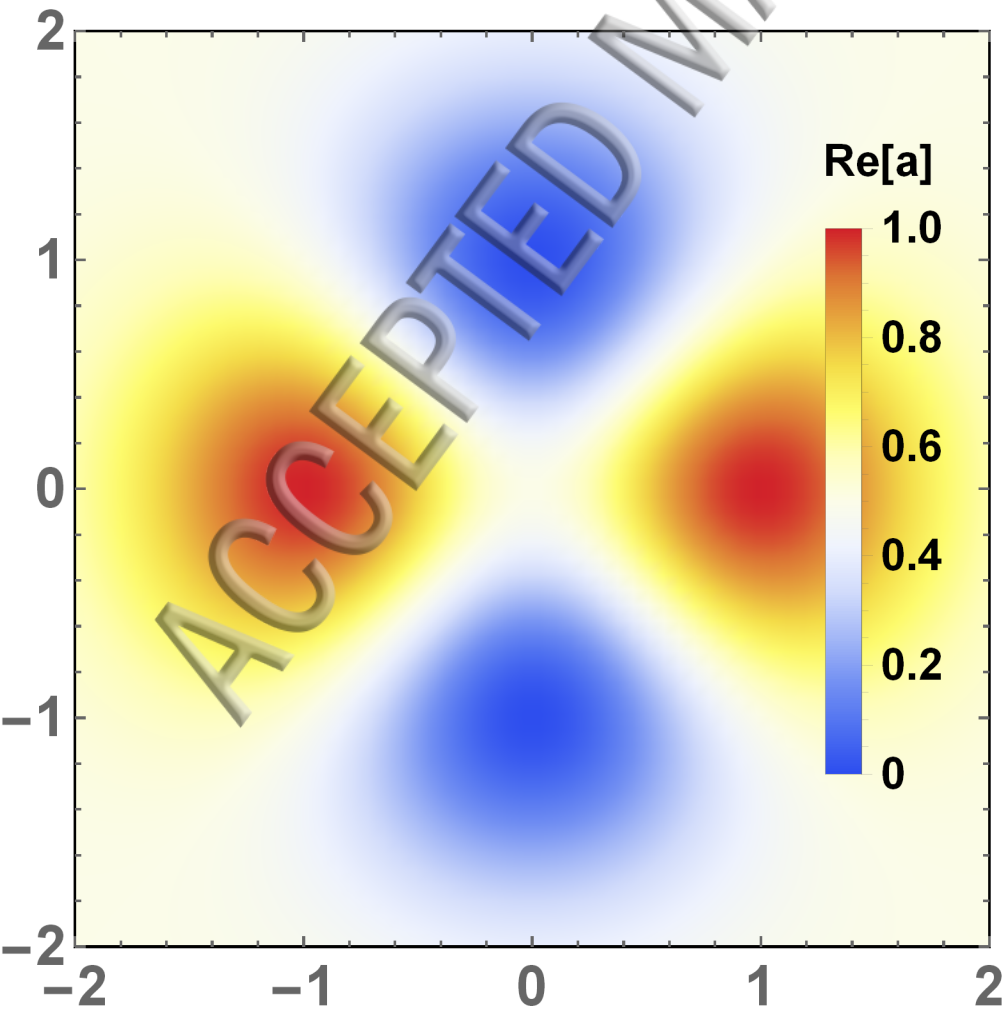

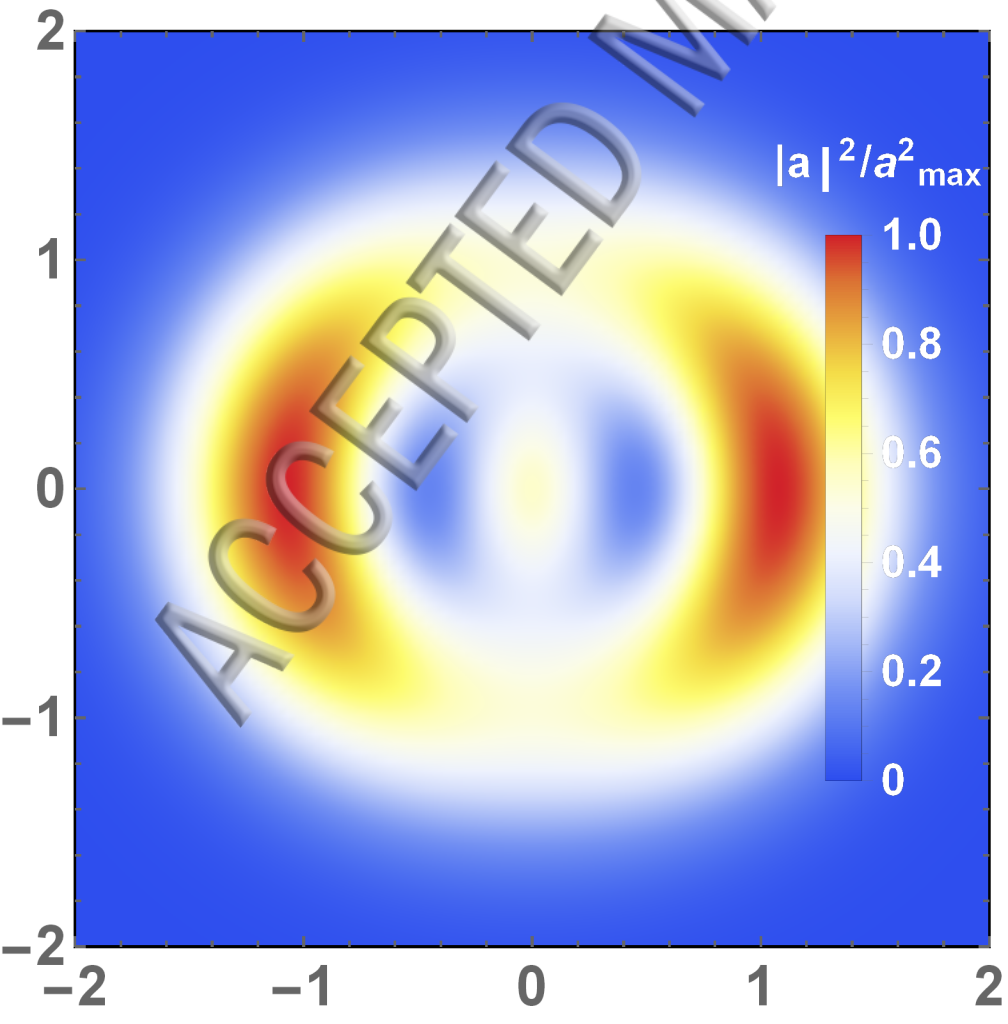

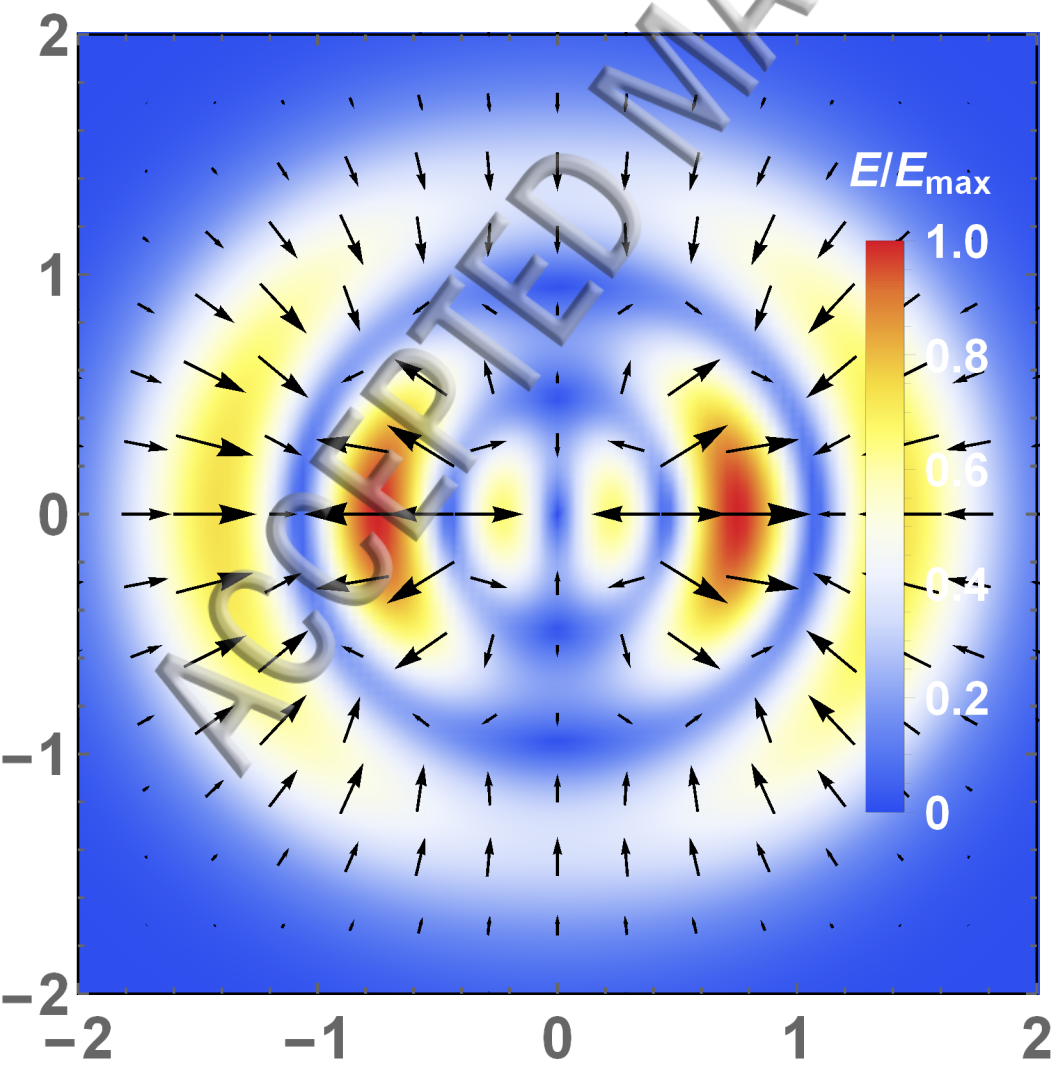

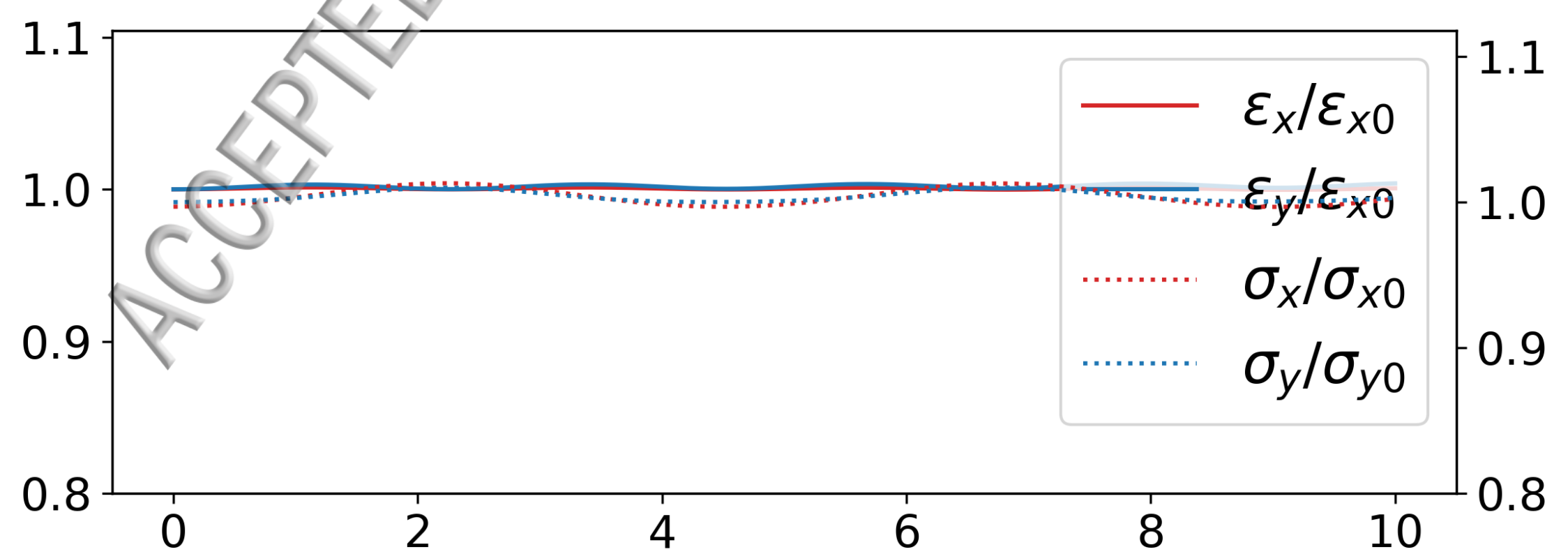
1.1
1.0
0.9
0.8
0
2
4
6
8
10
$\varepsilon_x/\varepsilon_{x0}$
$\varepsilon_y/\varepsilon_{x0}$
σ_x/σ_{x0}
σ_y/σ_{y0}

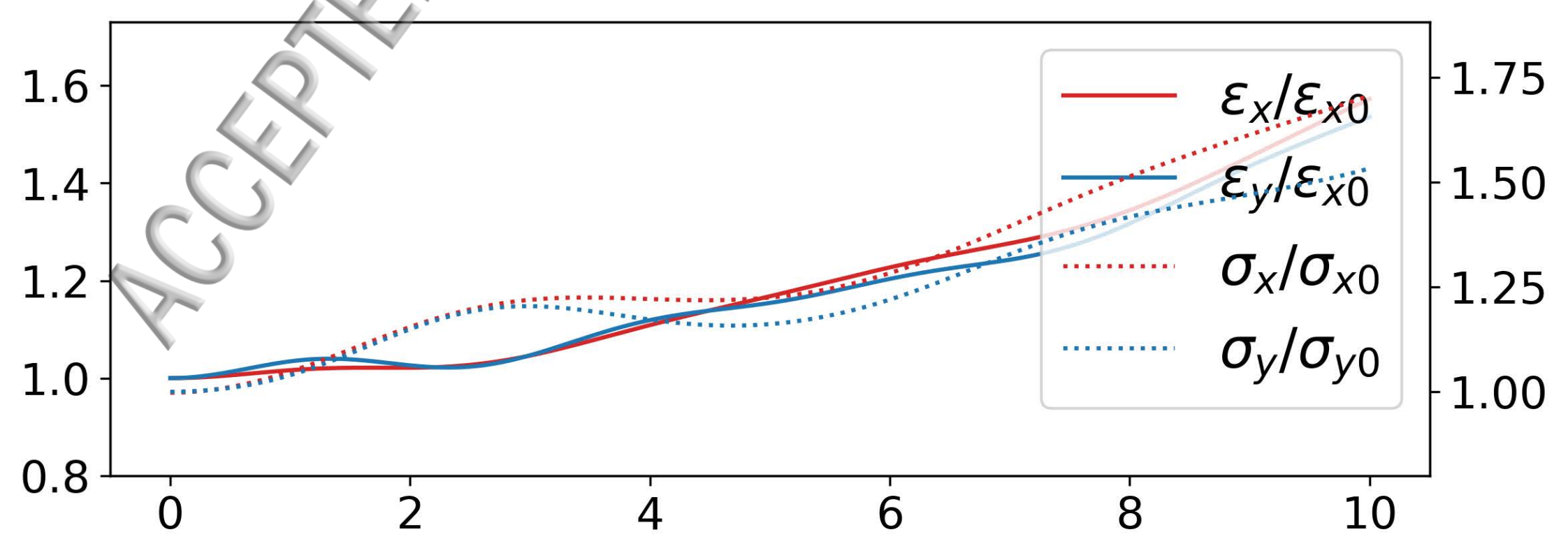
1.6
1.4
1.2
1.0
0.8
1.75
1.50
1.25
1.00
0
2
4
6
8
10
$\varepsilon_x/\varepsilon_{x0}$
$\varepsilon_y/\varepsilon_{x0}$
σ_x/σ_{x0}
σ_y/σ_{y0}

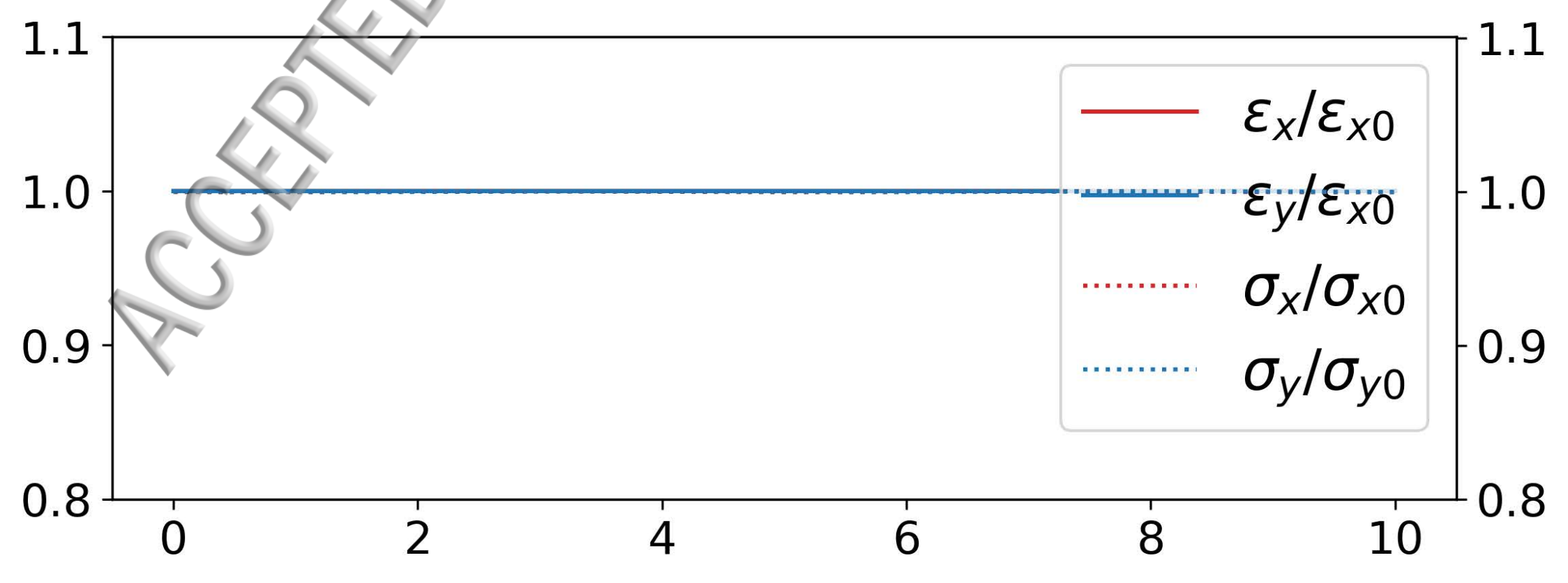
1.1
1.0
0.9
0.8
0
2
4
6
8
10
$\varepsilon_x/\varepsilon_{x0}$
$\varepsilon_y/\varepsilon_{x0}$
σ_x/σ_{x0}
σ_y/σ_{y0}

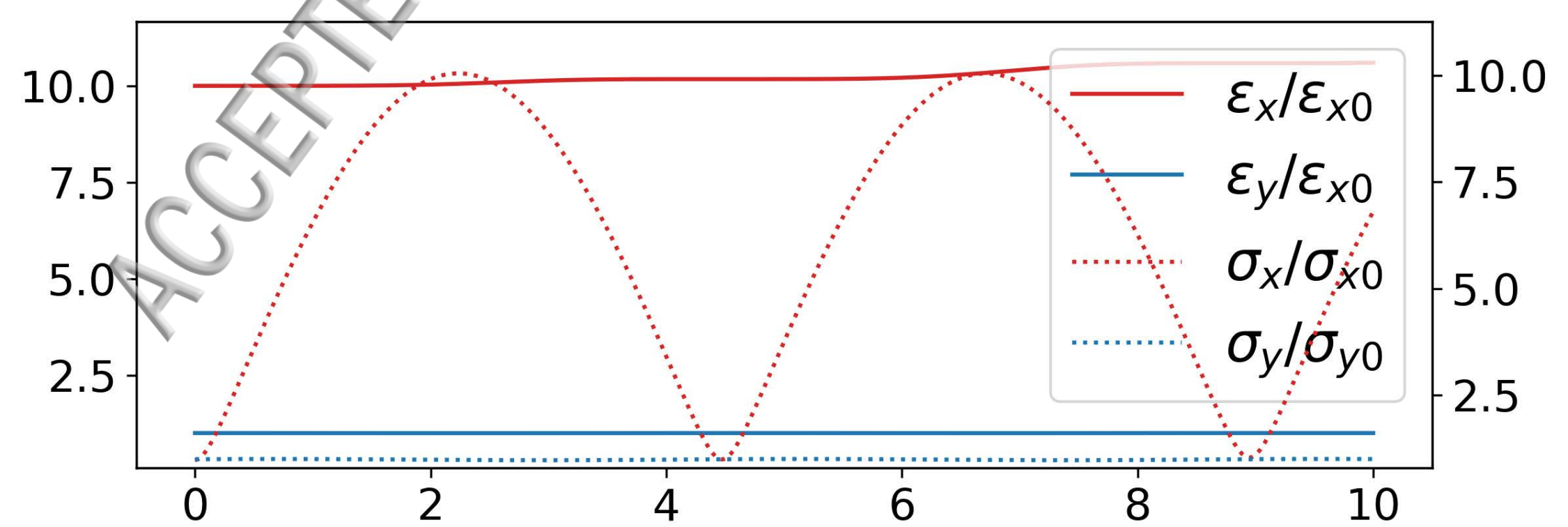
10.0
7.5
5.0
2.5
0
2
4
6
8
10
$\varepsilon_x/\varepsilon_{x0}$
$\varepsilon_y/\varepsilon_{x0}$
σ_x/σ_{x0}
σ_y/σ_{y0}

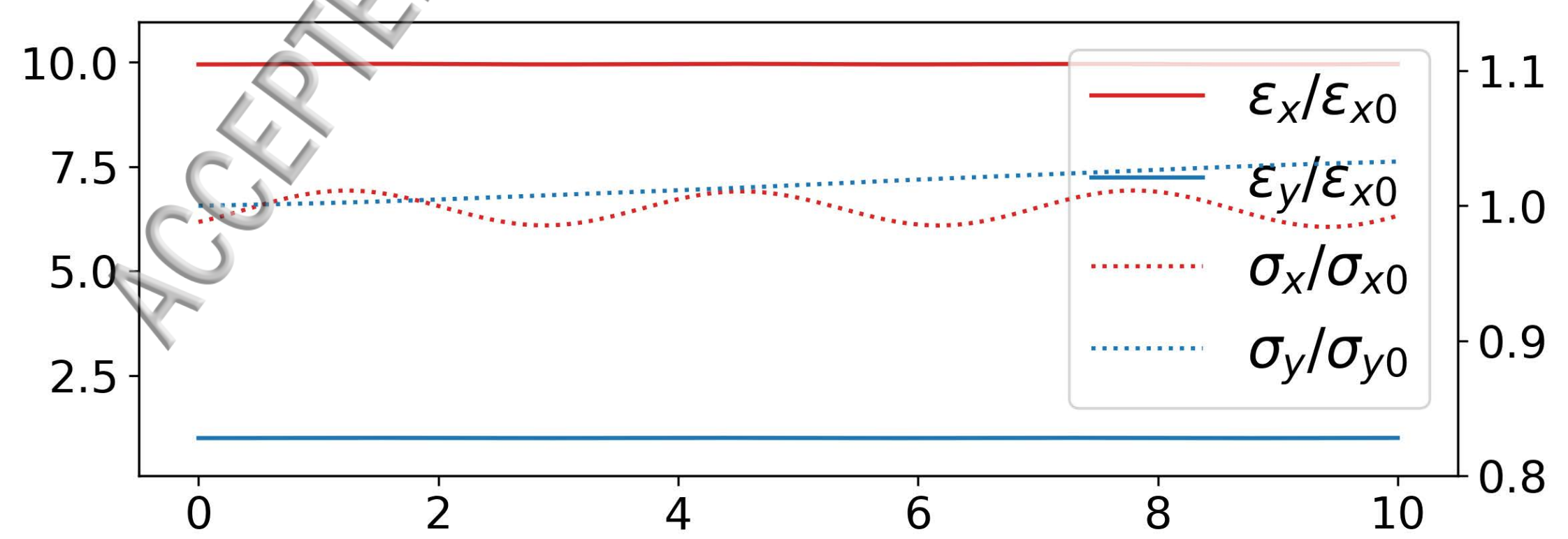
10.0
7.5
5.0
2.5
0
2
4
6
8
10
1.1
1.0
0.9
0.8
$\varepsilon_x/\varepsilon_{x0}$
$\varepsilon_y/\varepsilon_{x0}$
σ_x/σ_{x0}
σ_y/σ_{y0}

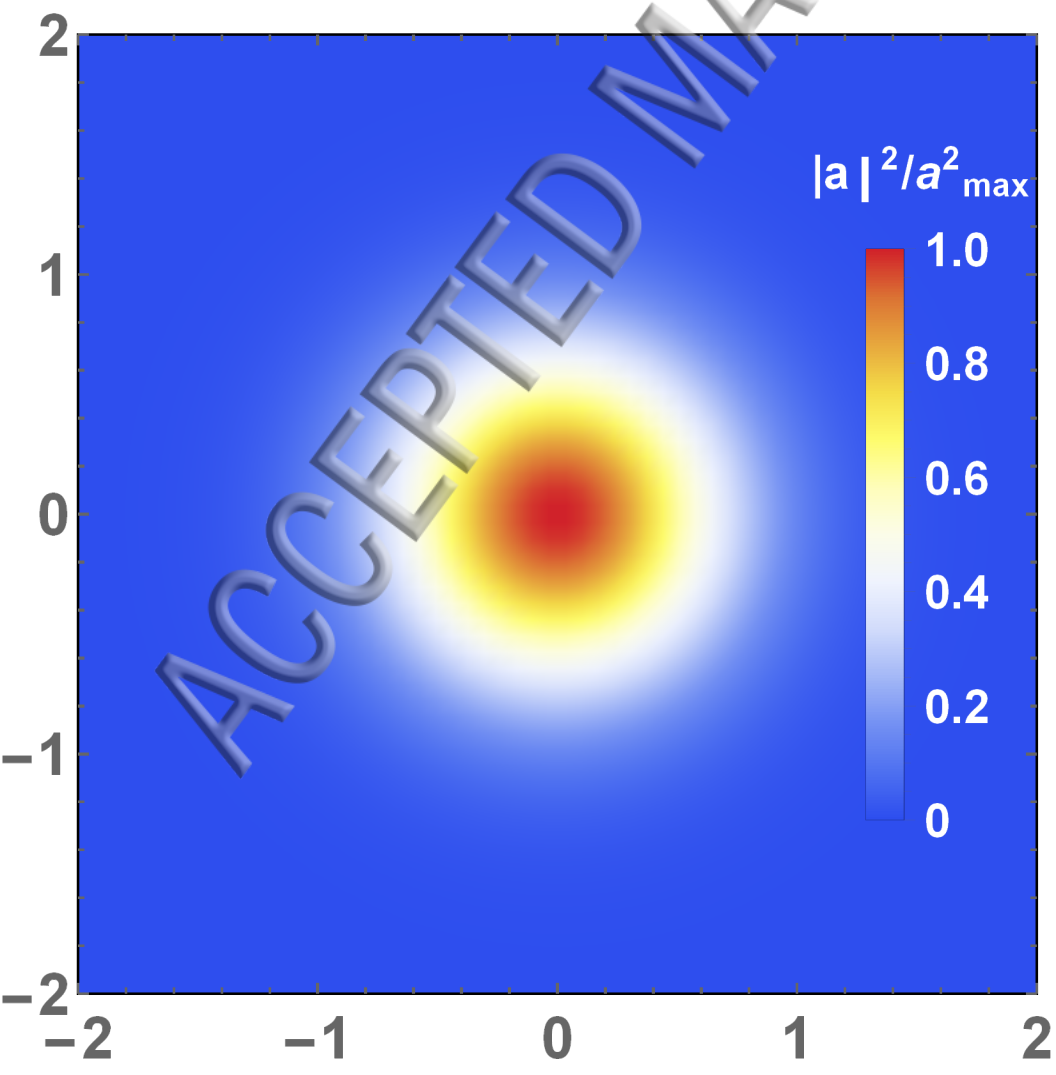

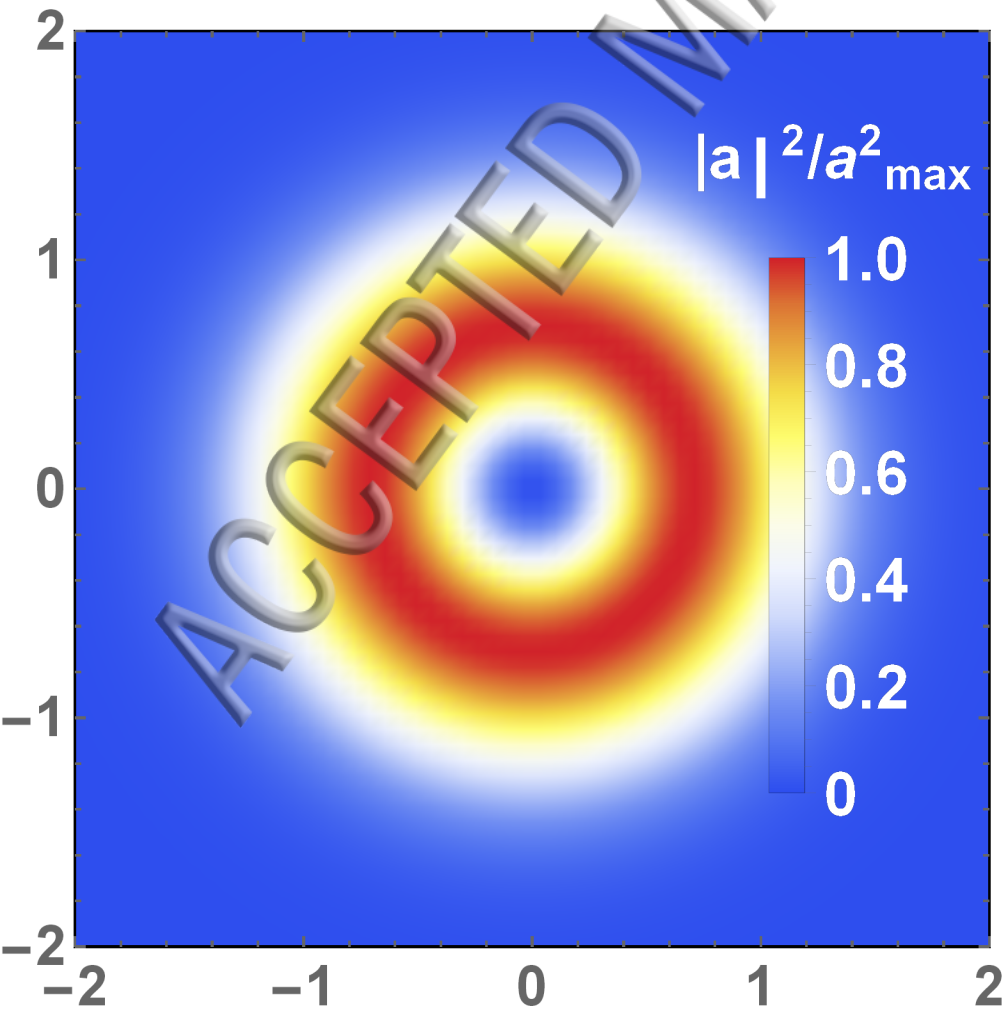

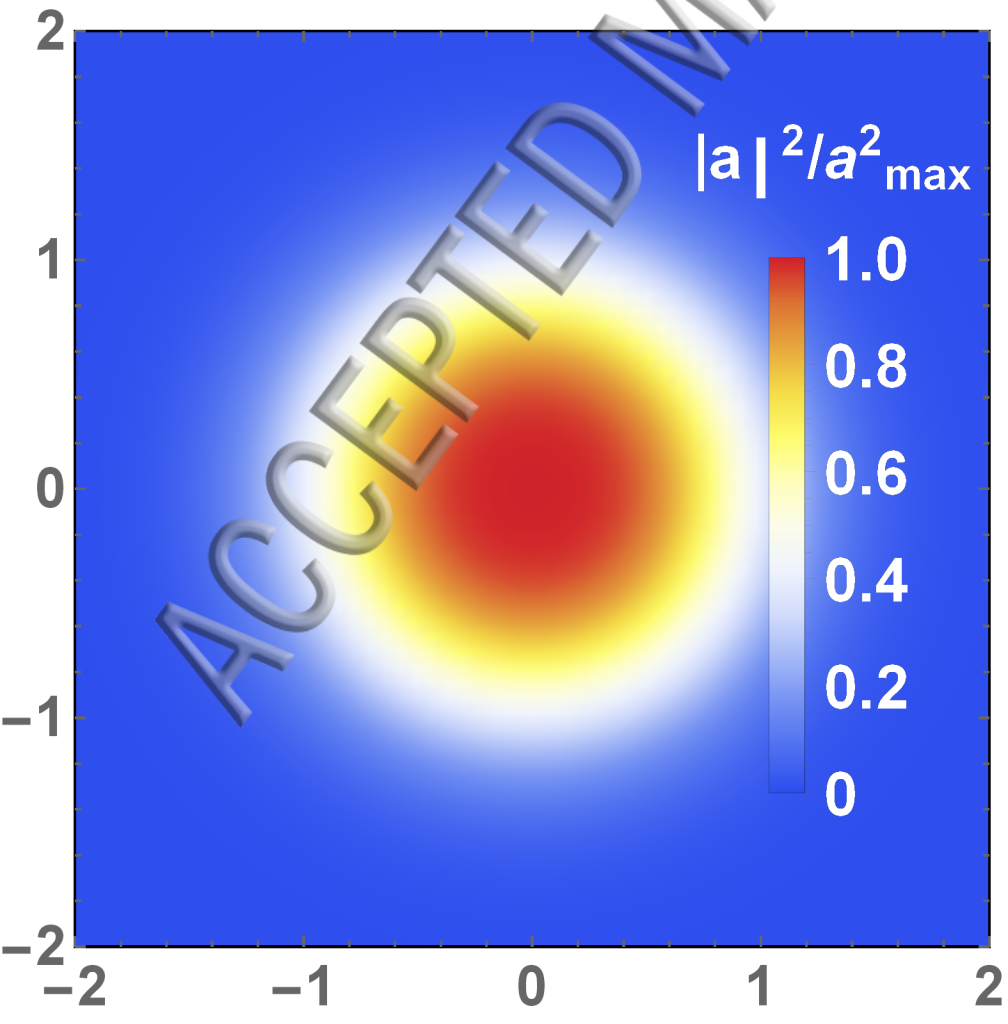

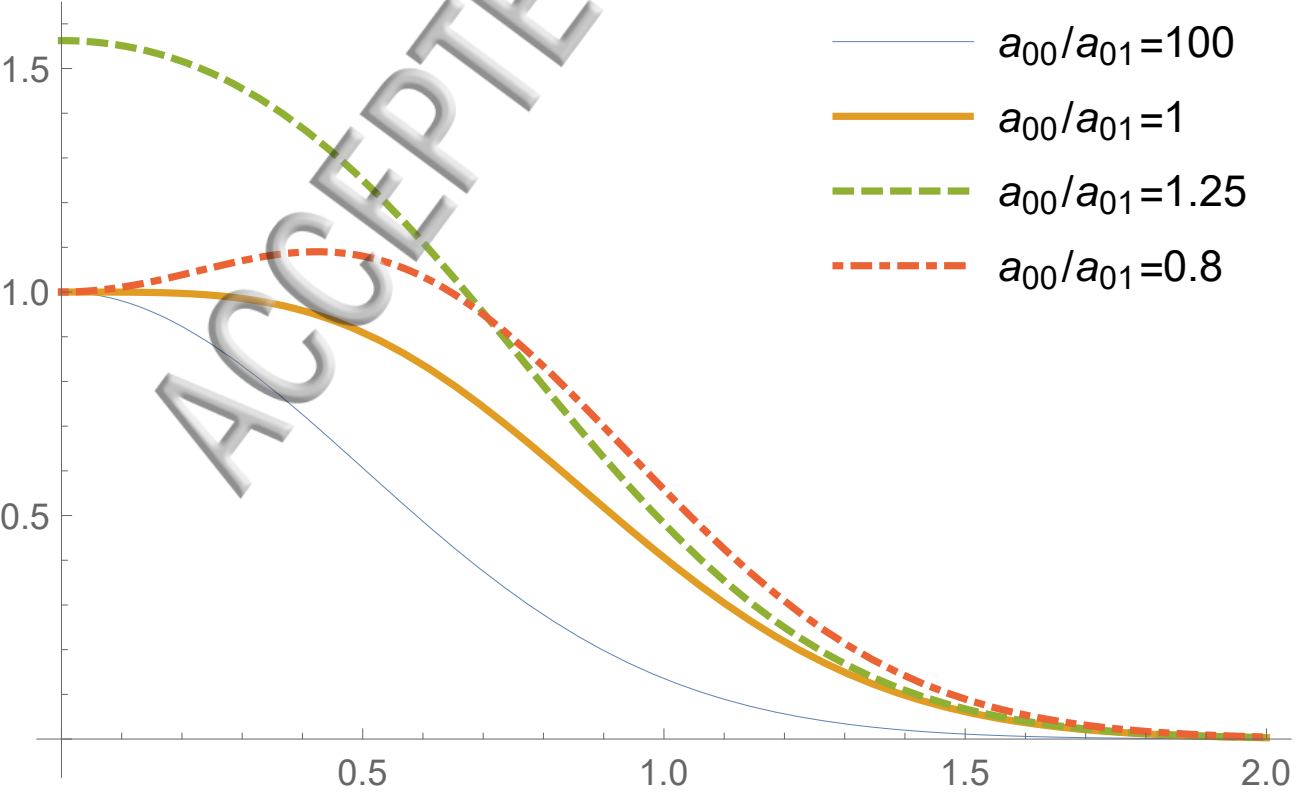

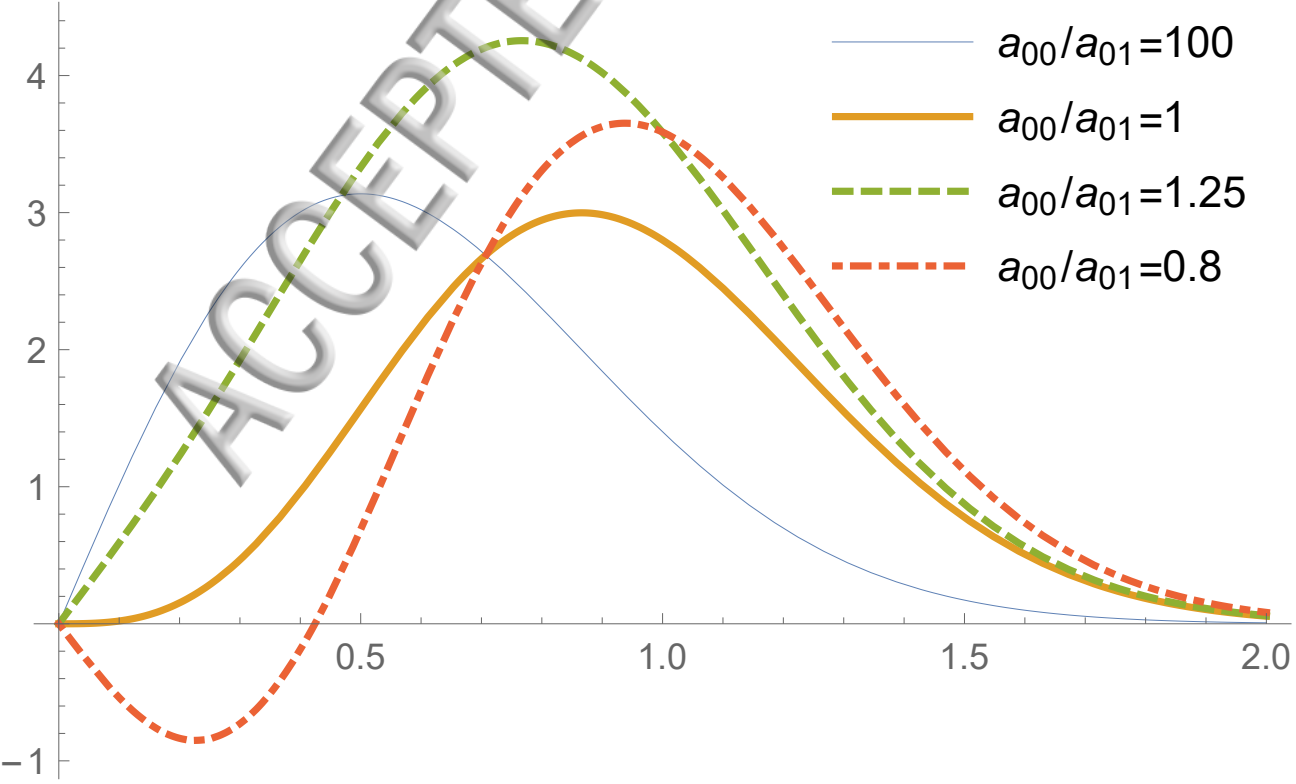

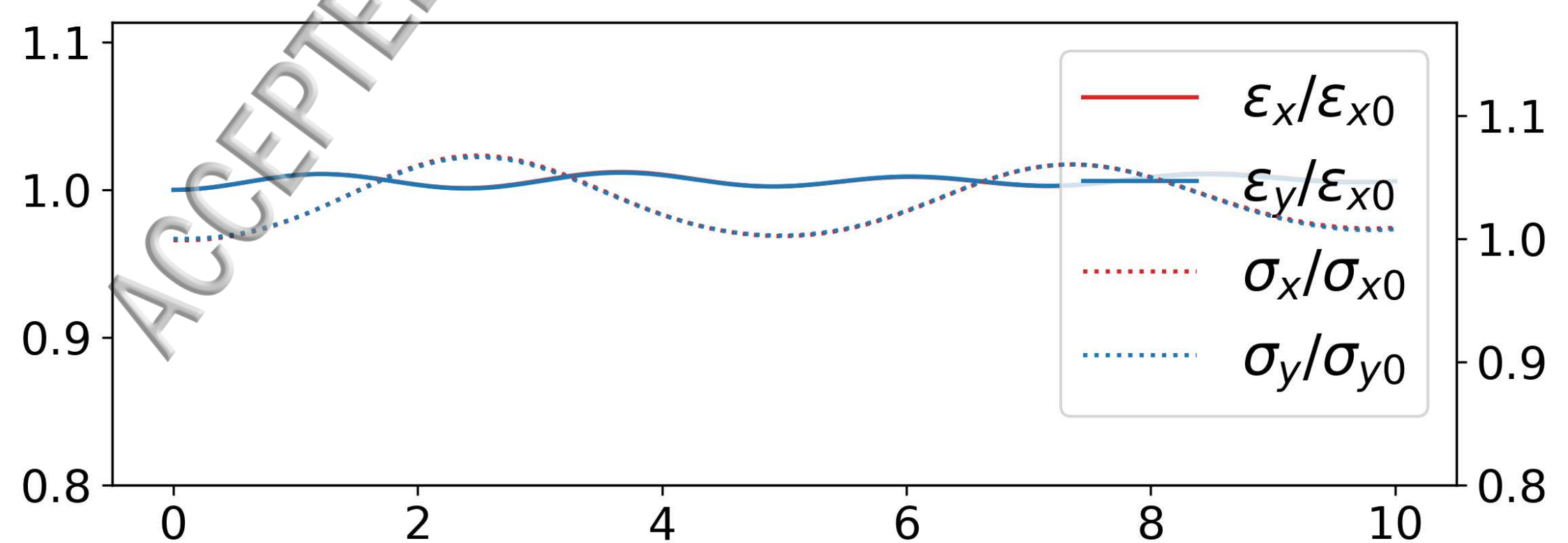
1.1
1.0
0.9
0.8
0
2
4
6
8
10
$\varepsilon_x/\varepsilon_{x0}$
$\varepsilon_y/\varepsilon_{x0}$
σ_x/σ_{x0}
σ_y/σ_{y0}

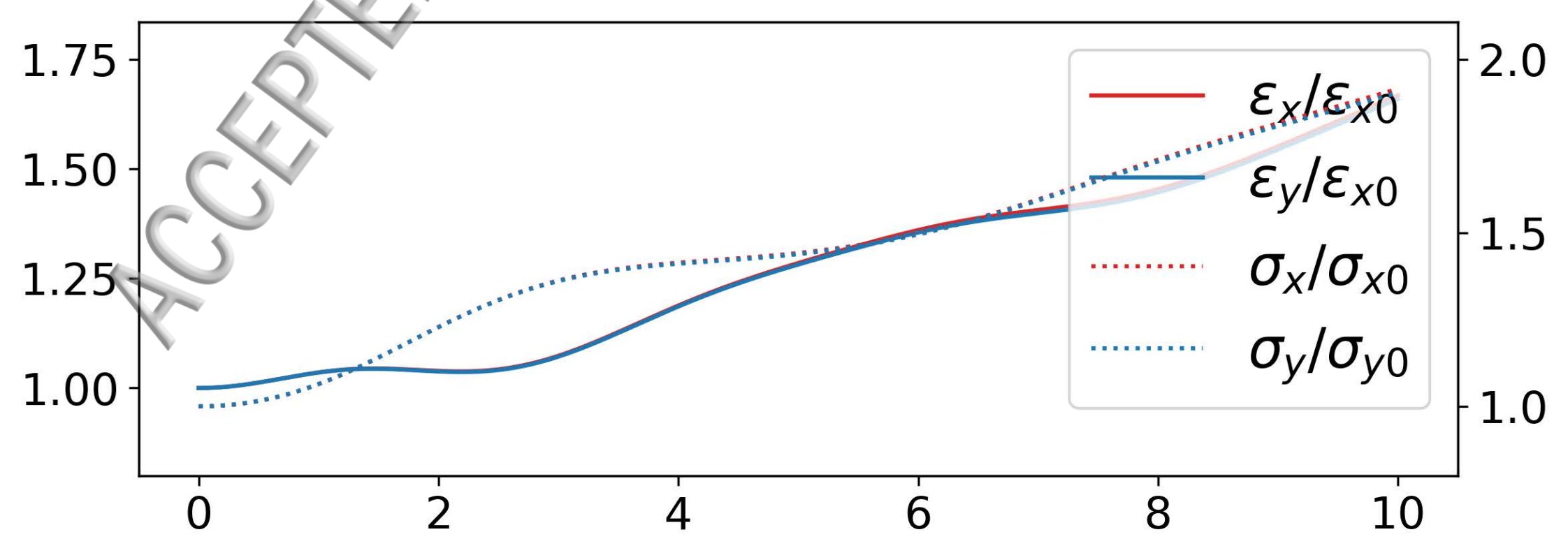
1.75
1.50
1.25
1.00
2.0
1.5
1.0
0
2
4
6
8
10
$\varepsilon_x/\varepsilon_{x0}$
$\varepsilon_y/\varepsilon_{x0}$
σ_x/σ_{x0}
σ_y/σ_{y0}

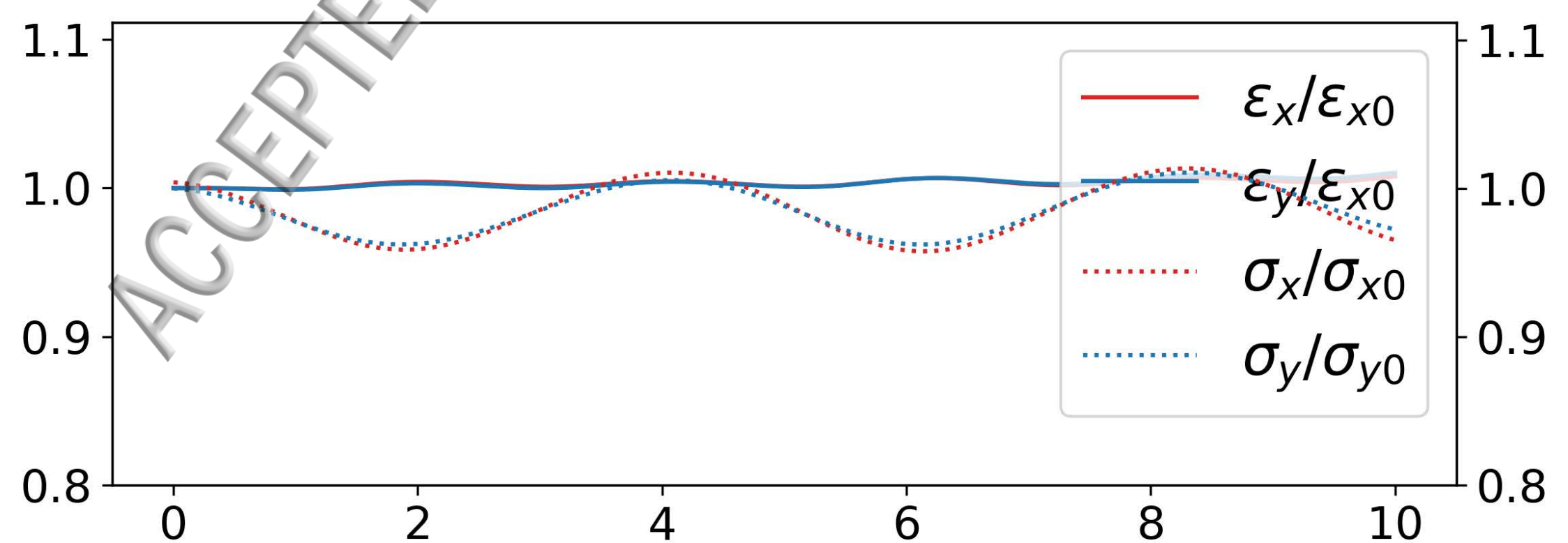
1.1
1.0
0.9
0.8
0
2
4
6
8
10
$\varepsilon_x/\varepsilon_{x0}$
$\varepsilon_y/\varepsilon_{x0}$
σ_x/σ_{x0}
σ_y/σ_{y0}